Available online at www.sciencedirect.com
ScienceDirect
Journal of Sound and Vibration 300 (2007) 1048–1070
JOURNAL OF SOUND AND VIBRATION
www.elsevier.com/locate/jsvi

Short Communication

A radial basis function approach for the free vibration analysis of functionally graded plates using a refined theory

C.M.C. Roque, A.J.M. Ferreira*, R.M.N. Jorge

Departamento de Engenharia Mecânica e Gestão Industrial, Faculdade de Engenharia da Universidade do Porto, Rua Dr. Roberto Frias, 4200-465 Porto, Portugal

Received 24 October 2005; received in revised form 27 June 2006; accepted 30 August 2006
Available online 27 October 2006

Abstract

The free vibration analysis of functionally graded plates is performed by the multiquadric radial basis function method and a higher-order shear deformation theory. The multiquadric method is a truly meshless method, allowing a fast and simple domain and boundary discretization. We use an homogenization technique for material properties based on the Mori–Tanaka scheme. Numerical tests show that the method is reliable and produces good results.

1. Introduction

In this paper, we use a meshless method based on radial basis functions for modelling functionally graded plates. The radial basis function method was first used by Hardy [1,2] for the interpolation of geographical scattered data and later used by Kansa [3,4] for the solution of partial differential equations (PDEs). Many other radial basis functions can be used as reviewed by Liu [5], Powell [6], Coleman [7], Sharan et al. [8], Wendland [9], among others. The method has also been applied to other engineering problems [10–12].

Recently the authors showed that the multiquadric method produces excellent results in static and free vibration analysis of beams and plates [13–15].

Functionally graded materials (FGMs) were first proposed by Bever and Duwez [16] in 1972. The computational modelling of FGMs is an important tool for the understanding of static and dynamic behavior, and has been the target of intense research, from micro- to macro-mechanics [17,18]. In this paper, we study the natural frequencies of several functionally graded plates. It has been illustrated that the use of higher-order theories [19] provides better accuracy for transverse shear stresses. In this paper, we use a

*Corresponding author. Tel.: +351 22 957 8713; fax: +351 22 953 7352.
E-mail address: ferreira@fe.up.pt (A.J.M. Ferreira).

0022-460X/$ - see front matter © 2006 Elsevier Ltd. All rights reserved.
doi:10.1016/j.jsv.2006.08.037

third-order theory of Pandya and Kant [20] that accounts for parabolic transverse shear stresses (at the cost of two extra rotations).

2. The problem

We consider a composite (functionally graded) plate with domain Ω bounded by a boundary $\partial\Omega$.

Let L and B be linear differential operators, being s and f functions defined in Ω and $\partial\Omega$:

$$Lu(\mathbf{x}) = s(\mathbf{x}), \quad \mathbf{x} \in \Omega, \tag{1}$$

$$Bu(\mathbf{x}) = f(\mathbf{x}), \quad \mathbf{x} \in \partial\Omega, \tag{2}$$

The classical laminated plate theory is not adequate for general analysis of composite plates, since it disregards the contribution of transverse shear stresses.

The first-order shear deformation theory assumes constant transverse shear deformations across the thickness of the plate. Therefore, shear correction factors are introduced to approximate the deformations to the real ones.

Higher-order shear deformation theories have the advantage of avoiding shear correction factors, because they assume a parabolic shear deformation across the thickness direction.

The theory of Reddy [19] is a five degree of freedom theory, with a cubic dependence of the in-plane displacements. It allows for zero transverse shear stresses at the top and bottom surfaces of the plate. As in Reddy's theory, the trigonometric theory of Arya [21] uses five degrees of freedom, but with a sine evolution of the displacements across the thickness of the plate.

In this paper, we use a displacement field with seven degrees of freedom by Pandya [20], which is reviewed in Section 3.

The plate is considered elastic, and nonlinear terms are discard from the strain–displacement relationships. From the principle of virtual work we obtain the equilibrium equations to be applied in Ω and the possible boundary conditions, applied in $\partial\Omega$. More details about boundary conditions are given in Section 4.

FGMs are composite materials with a smooth variation of the material properties. The objective of the gradient transitions is to smooth interlaminar stresses, a problem well known within laminar composite materials, where the material properties vary in an abrupt way. Functionally materials provide, within the same macroscopic material, a good balance between the individual properties of each constituent.

In this paper, we consider FGM plates with two constituents, ceramic and metal, with a variation of each constituent in the transverse direction. In order to indicate the content variation, we use a volume fraction function dependent on the transverse direction.

3. Higher-order theory

Pandya and co-workers [20] developed a successful theory that accounts for parabolic transverse shear stresses at the cost of two extra rotations. For a thick plate of thickness h, the displacement field is given by

$$\begin{aligned} u(x,y,z) &= u_0(x,y) + z\phi_x(x,y) + z^3\phi_x^*(x,y), \\ v(x,y,z) &= v_0(x,y) + z\phi_y(x,y) + z^3\phi_y^*(x,y), \\ w(x,y,z) &= w_0(x,y), \end{aligned} \tag{3}$$

where u and v are the in-plane displacements at any point (x,y,z), u_0 and v_0 denote the inplane displacement of the point $(x,y,0)$ on the midplane, w is the deflection, ϕ_x and ϕ_y are the rotations of the normals to the midplane about the y- and x-axis, respectively, and ϕ_x^*, ϕ_y^* are the higher-order rotational terms.

The strain–displacement relationships are given as

$$\begin{Bmatrix} \varepsilon_{xx} \\ \varepsilon_{yy} \\ \gamma_{xy} \\ \gamma_{xz} \\ \gamma_{yz} \end{Bmatrix} = \begin{Bmatrix} \dfrac{\partial u}{\partial x} \\ \dfrac{\partial v}{\partial y} \\ \dfrac{\partial u}{\partial y} + \dfrac{\partial v}{\partial x} \\ \dfrac{\partial u}{\partial z} + \dfrac{\partial w}{\partial x} \\ \dfrac{\partial v}{\partial z} + \dfrac{\partial w}{\partial y} \end{Bmatrix} \tag{4}$$

or by

$$\begin{Bmatrix} \varepsilon_{xx} \\ \varepsilon_{yy} \\ \gamma_{xy} \end{Bmatrix} = \begin{Bmatrix} \varepsilon_{xx}^{(0)} \\ \varepsilon_{yy}^{(0)} \\ \gamma_{xy}^{(0)} \end{Bmatrix} + z \begin{Bmatrix} \varepsilon_{xx}^{(1)} \\ \varepsilon_{yy}^{(1)} \\ \gamma_{xy}^{(1)} \end{Bmatrix} + z^3 \begin{Bmatrix} \varepsilon_{xx}^{(3)} \\ \varepsilon_{yy}^{(3)} \\ \gamma_{xy}^{(3)} \end{Bmatrix}, \tag{5}$$

$$\begin{Bmatrix} \gamma_{xz} \\ \gamma_{yz} \end{Bmatrix} = \begin{Bmatrix} \gamma_{xz}^{(0)} \\ \gamma_{yz}^{(0)} \end{Bmatrix} + z^2 \begin{Bmatrix} \gamma_{xz}^{(2)} \\ \gamma_{yz}^{(2)} \end{Bmatrix}, \tag{6}$$

where the strain components are obtained as

$$\begin{Bmatrix} \varepsilon_{xx}^{(0)} \\ \varepsilon_{yy}^{(0)} \\ \gamma_{xy}^{(0)} \end{Bmatrix} = \begin{Bmatrix} \dfrac{\partial u_0}{\partial x} \\ \dfrac{\partial v_0}{\partial y} \\ \dfrac{\partial u_0}{\partial y} + \dfrac{\partial v_0}{\partial x} \end{Bmatrix}, \quad \begin{Bmatrix} \varepsilon_{xx}^{(1)} \\ \varepsilon_{yy}^{(1)} \\ \gamma_{xy}^{(1)} \end{Bmatrix} = \begin{Bmatrix} \dfrac{\partial \phi_x}{\partial x} \\ \dfrac{\partial \phi_y}{\partial y} \\ \dfrac{\partial \phi_x}{\partial y} + \dfrac{\partial \phi_y}{\partial x} \end{Bmatrix}, \quad \begin{Bmatrix} \varepsilon_{xx}^{(3)} \\ \varepsilon_{yy}^{(3)} \\ \gamma_{xy}^{(3)} \end{Bmatrix} = \begin{Bmatrix} \dfrac{\partial \phi_x^*}{\partial x} \\ \dfrac{\partial \phi_y^*}{\partial y} \\ \dfrac{\partial \phi_x^*}{\partial y} + \dfrac{\partial \phi_y^*}{\partial x} \end{Bmatrix}, \tag{7}$$

$$\begin{Bmatrix} \gamma_{xz}^{(0)} \\ \gamma_{yz}^{(0)} \end{Bmatrix} = \begin{Bmatrix} \dfrac{\partial w_0}{\partial x} + \phi_x \\ \dfrac{\partial w_0}{\partial y} + \phi_y \end{Bmatrix}, \quad \begin{Bmatrix} \gamma_{xz}^{(2)} \\ \gamma_{yz}^{(2)} \end{Bmatrix} = \begin{Bmatrix} \phi_x^* \\ \phi_y^* \end{Bmatrix}. \tag{8}$$

By neglecting transverse normal stress, σ_z, in each orthotropic layer, the stress–strain relations in the local (material) Cartesian system can be obtained as

$$\begin{Bmatrix} \sigma_1 \\ \sigma_2 \\ \tau_{12} \\ \tau_{23} \\ \tau_{31} \end{Bmatrix} = \begin{bmatrix} Q_{11} & Q_{12} & 0 & 0 & 0 \\ Q_{12} & Q_{22} & 0 & 0 & 0 \\ 0 & 0 & Q_{33} & 0 & 0 \\ 0 & 0 & 0 & Q_{44} & 0 \\ 0 & 0 & 0 & 0 & Q_{55} \end{bmatrix} \begin{Bmatrix} \varepsilon_1 \\ \varepsilon_2 \\ \gamma_{12} \\ \gamma_{23} \\ \gamma_{31} \end{Bmatrix}, \tag{9}$$

where subscripts 1 and 2 are, respectively, the fiber and the normal to fiber inplane directions, and 3 is the direction normal to the plate. The reduced stiffness components, Q_{ij} are given by

$$Q_{11} = \frac{E_1}{1 - \nu_{12}\nu_{21}}, \quad Q_{22} = \frac{E_2}{1 - \nu_{12}\nu_{21}}, \quad Q_{12} = \nu_{21} Q_{11},$$

$$Q_{33} = G_{12}, \quad Q_{44} = G_{23}, \quad Q_{55} = G_{31},$$
$$v_{21} = v_{12}\frac{E_2}{E_1}, \tag{10}$$

in which E_1, E_2, v_{12}, G_{12}, G_{23} and G_{31} are material properties of the lamina. Shear correction factors are not needed in this formulation due to third-order evolution of displacements with the thickness coordinate.

Relations (9) can now be transformed into global (plate) Cartesian system by coordinate transformation as [19]

$$\begin{Bmatrix} \sigma_{xx} \\ \sigma_{yy} \\ \tau_{xy} \\ \tau_{yz} \\ \tau_{zx} \end{Bmatrix} = \begin{bmatrix} \overline{Q}_{11} & \overline{Q}_{12} & \overline{Q}_{13} & 0 & 0 \\ \overline{Q}_{12} & \overline{Q}_{22} & \overline{Q}_{23} & 0 & 0 \\ \overline{Q}_{13} & \overline{Q}_{23} & \overline{Q}_{33} & 0 & 0 \\ 0 & 0 & 0 & \overline{Q}_{44} & \overline{Q}_{45} \\ 0 & 0 & 0 & \overline{Q}_{45} & \overline{Q}_{55} \end{bmatrix} \begin{Bmatrix} \varepsilon_{xx} \\ \varepsilon_{yy} \\ \gamma_{xy} \\ \gamma_{yz} \\ \gamma_{zx} \end{Bmatrix}. \tag{11}$$

The governing equations are derived from the principle of Hamilton. The virtual strain energy (δU), the virtual work done by applied forces (δV) and virtual kinetic energy (δK) are given by

$$\begin{aligned} \delta U = & \int_{\Omega_0} \left\{ \int_{-h/2}^{h/2} [\sigma_{xx}(\delta\varepsilon_{xx}^{(0)} + z\delta\varepsilon_{xx}^{(1)} + z^3\delta\varepsilon_{xx}^{(3)}) + \sigma_{yy}(\delta\varepsilon_{yy}^{(0)} + z\delta\varepsilon_{yy}^{(1)} + z^3\delta\varepsilon_{yy}^{(3)}) \right. \\ & \left. + \tau_{xy}(\delta\gamma_{xy}^{(0)} + z\delta\gamma_{xy}^{(1)} + z^3\delta\gamma_{xy}^{(3)}) + \tau_{xz}(\delta\gamma_{xz}^{(0)} + z^2\delta\gamma_{xz}^{(2)}) + \tau_{yz}(\delta\gamma_{yz}^{(0)} + z^2\delta\gamma_{yz}^{(2)})] \, \mathrm{d}z \right\} \mathrm{d}x \, \mathrm{d}y \\ = & \int_{\Omega_0} (N_{xx}\delta\varepsilon_{xx}^{(0)} + M_{xx}\delta\varepsilon_{xx}^{(1)} + S_{xx}\delta\varepsilon_{xx}^{(3)} + N_{yy}\delta\varepsilon_{yy}^{(0)} + M_{yy}\delta\varepsilon_{yy}^{(1)} + S_{yy}\delta\varepsilon_{yy}^{(3)} + N_{xy}\delta\gamma_{xy}^{(0)} \\ & + M_{xy}\delta\gamma_{xy}^{(1)} + S_{xy}\delta\gamma_{xy}^{(3)} + Q_{xz}\delta\gamma_{xz}^{(0)} + 3T_{xz}\delta\gamma_{xz}^{(2)} + Q_{yz}\delta\gamma_{yz}^{(0)} + 3T_{yz}\delta\gamma_{yz}^{(2)}) \, \mathrm{d}x \, \mathrm{d}y, \end{aligned} \tag{12}$$

$$\delta V = -\int_{\Omega_0} q\delta w_0 \, \mathrm{d}x \, \mathrm{d}y, \tag{13}$$

$$\begin{aligned} \delta K = & \int_{\Omega_0} \left\{ \int_{-h/2}^{h/2} \rho(\dot{u}\delta\dot{u} + \dot{v}\delta\dot{v} + \dot{w}\delta\dot{w}) \, \mathrm{d}z \right\} \mathrm{d}x \, \mathrm{d}y \\ = & \int_{\Omega_0} \{I_0(\dot{u}\delta\dot{u} + \dot{v}\delta\dot{v} + \dot{w}\delta\dot{w}) + I_1(\dot{\phi}_x\delta\dot{u} + \dot{u}\delta\dot{\phi}_x + \dot{\phi}_y\delta\dot{v} + \dot{v}\delta\dot{\phi}_y) + I_2(\dot{\phi}_x\delta\dot{\phi}_x + \dot{\phi}_y\delta\dot{\phi}_y) \\ & + I_3(\dot{\phi}_x^*\delta\dot{u} + \dot{u}\delta\dot{\phi}_x^* + \dot{\phi}_y^*\delta\dot{v} + \dot{v}\delta\dot{\phi}_y^*) + I_4(\dot{\phi}_x^*\delta\dot{\phi}_x + \dot{\phi}_x\delta\dot{\phi}_x^* + \dot{\phi}_y^*\delta\dot{\phi}_y + \dot{\phi}_y\delta\dot{\phi}_y^*) \\ & + I_6(\dot{\phi}_x^*\delta\dot{\phi}_x^* + \dot{\phi}_y^*\delta\dot{\phi}_y^*)\} \, \mathrm{d}x \, \mathrm{d}y, \end{aligned} \tag{14}$$

where Ω_0 denotes the midplane domain of the laminate, q is the external distributed load being the stress resultants and moments given by

$$\begin{Bmatrix} N_{\alpha\beta} \\ M_{\alpha\beta} \\ S_{\alpha\beta} \end{Bmatrix} = \int_{-h/2}^{h/2} \sigma_{\alpha\beta} \begin{Bmatrix} 1 \\ z \\ z^3 \end{Bmatrix} \mathrm{d}z. \tag{15}$$

First- and higher-order transverse resultants are given by

$$\begin{Bmatrix} Q_{\alpha z} \\ T_{\alpha z} \end{Bmatrix} = \int_{-h/2}^{h/2} \sigma_{\alpha z} \begin{Bmatrix} 1 \\ z^2 \end{Bmatrix} \mathrm{d}z \tag{16}$$

and the inertia terms are

$$I_i = \int_{-h/2}^{h/2} \rho z^i \, \mathrm{d}z, \quad i = 1, 2, 3, 4, 6, \tag{17}$$

where α, β take the symbols x, y.

Substituting for $\delta U, \delta V$ and δK, into the virtual work statement, noting that the virtual strains can be expressed in terms of the generalized displacements, integrating by parts to relieve from any derivatives of the generalized displacements and using the fundamental lemma of the calculus of variations, we obtain the equations of motion

$$\frac{\partial N_{xx}}{\partial x} + \frac{\partial N_{xy}}{\partial y} = I_0 \ddot{u}_0 + I_1 \ddot{\phi}_x + I_3 \ddot{\phi}_x^*, \tag{18a}$$

$$\frac{\partial N_{yy}}{\partial y} + \frac{\partial N_{xy}}{\partial x} = I_0 \ddot{v}_0 + I_1 \ddot{\phi}_y + I_3 \ddot{\phi}_y^*, \tag{18b}$$

$$\frac{\partial Q_{xz}}{\partial x} + \frac{\partial Q_{yz}}{\partial y} + q = I_0 \ddot{w}_0, \tag{18c}$$

$$\frac{\partial M_{xx}}{\partial x} + \frac{\partial M_{xy}}{\partial y} - Q_{xz} = I_1 \ddot{u}_0 + I_2 \ddot{\phi}_x + I_4 \ddot{\phi}_x^*, \tag{18d}$$

$$\frac{\partial M_{yy}}{\partial y} + \frac{\partial M_{xy}}{\partial x} - Q_{yz} = I_1 \ddot{v}_0 + I_2 \ddot{\phi}_y + I_4 \ddot{\phi}_y^*, \tag{18e}$$

$$\frac{\partial S_{xx}}{\partial x} + \frac{\partial S_{xy}}{\partial y} - 3T_{xz} = I_3 \ddot{u}_0 + I_4 \ddot{\phi}_x + I_6 \ddot{\phi}_x^*, \tag{18f}$$

$$\frac{\partial S_{yy}}{\partial y} + \frac{\partial S_{xy}}{\partial x} - 3T_{yz} = I_3 \ddot{v}_0 + I_4 \ddot{\phi}_y + I_6 \ddot{\phi}_y^*. \tag{18g}$$

The equations of motion can now be written in terms of the displacements by substituting strains and stress resultants into these equations. These equations are detailed in Appendix A.

4. Boundary conditions

We consider three types of boundary conditions, simply supported (S), clamped (C) and free (F). At a point $a(x, 0)$, the boundary conditions are described as

$$\begin{aligned}
&S: u(a) = 0; \quad w(a) = 0; \quad \phi_x(a) = 0; \quad \phi_x^*(a) = 0; \quad N_{yy}(a) = 0; \quad M_{yy}(a) = 0; \quad S_{yy}(a) = 0,\\
&C: u(a) = 0; \quad v(a) = 0; \quad w(a) = 0; \quad \phi_x(a) = 0; \quad \phi_x^*(a) = 0; \quad \phi_y(a) = 0; \quad \phi_y^*(a) = 0,\\
&F: N_{yy}(a) = 0; \quad N_{xy}(a) = 0; \quad M_{yy}(a) = 0; \quad M_{xy}(a) = 0; \quad S_{yy}(a) = 0; \quad S_{xy}(a) = 0; \quad Q_{yz}(a) = 0,
\end{aligned}$$

where the generalized resultants are given by

$$\begin{aligned}
N_{yy} = {} & A_{12}\frac{\partial u}{\partial x} + A_{22}\frac{\partial v}{\partial y} + A_{23}\left(\frac{\partial u}{\partial y} + \frac{\partial v}{\partial x}\right) + B_{12}\frac{\partial \phi_x}{\partial x} + B_{22}\frac{\partial \phi_y}{\partial y} + B_{23}\left(\frac{\partial \phi_x}{\partial y} + \frac{\partial \phi_y}{\partial x}\right)\\
& + E_{12}\frac{\partial \phi_x^*}{\partial x} + E_{22}\frac{\partial \phi_y^*}{\partial y} + E_{23}\left(\frac{\partial \phi_x^*}{\partial y} + \frac{\partial \phi_y^*}{\partial x}\right),
\end{aligned} \tag{19}$$

$$N_{xy} = A_{13}\frac{\partial u}{\partial x} + A_{23}\frac{\partial v}{\partial y} + A_{33}\left(\frac{\partial u}{\partial y} + \frac{\partial v}{\partial x}\right) + B_{13}\frac{\partial \phi_x}{\partial x} + B_{23}\frac{\partial \phi_y}{\partial y} + B_{33}\left(\frac{\partial \phi_x}{\partial y} + \frac{\partial \phi_y}{\partial x}\right) + E_{13}\frac{\partial \phi_x^*}{\partial x} + E_{23}\frac{\partial \phi_y^*}{\partial y} + E_{33}\left(\frac{\partial \phi_x^*}{\partial y} + \frac{\partial \phi_y^*}{\partial x}\right), \tag{20}$$

$$M_{yy} = B_{12}\frac{\partial u}{\partial x} + B_{22}\frac{\partial v}{\partial y} + B_{23}\left(\frac{\partial u}{\partial y} + \frac{\partial v}{\partial x}\right) + F_{12}\frac{\partial \phi_x}{\partial x} + F_{22}\frac{\partial \phi_y}{\partial y} + F_{23}\left(\frac{\partial \phi_x}{\partial y} + \frac{\partial \phi_y}{\partial x}\right) + G_{12}\frac{\partial \phi_x^*}{\partial x} + G_{22}\frac{\partial \phi_y^*}{\partial y} + G_{23}\left(\frac{\partial \phi_x^*}{\partial y} + \frac{\partial \phi_y^*}{\partial x}\right), \tag{21}$$

$$M_{xy} = B_{13}\frac{\partial u}{\partial x} + B_{23}\frac{\partial v}{\partial y} + B_{33}\left(\frac{\partial u}{\partial y} + \frac{\partial v}{\partial x}\right) + F_{13}\frac{\partial \phi_x}{\partial x} + F_{23}\frac{\partial \phi_y}{\partial y} + F_{33}\left(\frac{\partial \phi_x}{\partial y} + \frac{\partial \phi_y}{\partial x}\right) + G_{13}\frac{\partial \phi_x^*}{\partial x} + G_{23}\frac{\partial \phi_y^*}{\partial y} + G_{33}\left(\frac{\partial \phi_x^*}{\partial y} + \frac{\partial \phi_y^*}{\partial x}\right), \tag{22}$$

$$S_{yy} = E_{12}\frac{\partial u}{\partial x} + E_{22}\frac{\partial v}{\partial y} + E_{23}\left(\frac{\partial u}{\partial y} + \frac{\partial v}{\partial x}\right) + G_{12}\frac{\partial \phi_x}{\partial x} + G_{22}\frac{\partial \phi_y}{\partial y} + G_{23}\left(\frac{\partial \phi_x}{\partial y} + \frac{\partial \phi_y}{\partial x}\right) + H_{12}\frac{\partial \phi_x^*}{\partial x} + H_{22}\frac{\partial \phi_y^*}{\partial y} + H_{23}\left(\frac{\partial \phi_x^*}{\partial y} + \frac{\partial \phi_y^*}{\partial x}\right), \tag{23}$$

$$S_{xy} = E_{13}\frac{\partial u}{\partial x} + E_{23}\frac{\partial v}{\partial y} + E_{33}\left(\frac{\partial u}{\partial y} + \frac{\partial v}{\partial x}\right) + G_{13}\frac{\partial \phi_x}{\partial x} + G_{23}\frac{\partial \phi_y}{\partial y} + G_{33}\left(\frac{\partial \phi_x}{\partial y} + \frac{\partial \phi_y}{\partial x}\right) + H_{13}\frac{\partial \phi_x^*}{\partial x} + H_{23}\frac{\partial \phi_y^*}{\partial y} + H_{33}\left(\frac{\partial \phi_x^*}{\partial y} + \frac{\partial \phi_y^*}{\partial x}\right), \tag{24}$$

$$Q_{yz} = I_{44}\left(\phi_y + \frac{\partial w}{\partial y}\right) + I_{45}\left(\phi_x + \frac{\partial w}{\partial x}\right) + 3K_{44}\phi_y^* + 3K_{45}\phi_x^*. \tag{25}$$

5. The multiquadric approach

Consider N_I distinct nodes in domain $\Omega\backslash\partial\Omega$ and N_B distinct nodes on a boundary $\partial\Omega$. A multiquadric function (g) is defined as

$$g(r, c) = (\|x - x_j\|^2 + c^2)^{1/2} \tag{26}$$

where r is the Euclidean distance between two nodes and c is a shape parameter that improves the function surface so that convergence gets faster [3,4,22–25]. Although other radial basis functions could be used (Gaussians, splines, etc.), multiquadrics have proved to be excellent for global, smooth, boundary-value problems, such as plates in bending.

We interpolate a function $\mathbf{u}(\mathbf{x})$ as

$$\mathbf{u} \simeq \bar{\mathbf{u}} = \sum_{j=1}^{N} \alpha_j g_j, \tag{27}$$

where α_j are parameters to be determined after the collocation method is applied, and $N = N_I + N_B$. We consider a global collocation method where the linear operators L and B act in domain $\Omega\backslash\partial\Omega$ and boundary $\partial\Omega$ define a set of global equations in the form

$$\begin{pmatrix} L_{ii}(g) & L_{ib}(g) \\ B_{bi}(g) & B_{bb}(g) \end{pmatrix} \begin{pmatrix} \alpha_i \\ \alpha_b \end{pmatrix} = \begin{pmatrix} f_i \\ s_b \end{pmatrix}, \tag{28}$$

where i and b denote domain and boundary nodes, respectively; f_i and f_b are some external conditions in domain and boundary. In bending plates these can be external forces, and in free vibration analysis, they will both be zero.

The use of shape parameters is a difficult task, not yet solved. The choice of the shape parameter influences the quality of the solution, the conditioning of the coefficient matrix and the stability of the method. Various methods have tried to obviate this problem, in particular in papers of Kansa [22], Hon and colleagues [26,27], and Rippa [28], who introduced an optimization technique. We use a constant shape parameter $c = 6d$, where d is the distance between two consecutive nodes. Our numerical experience shows that a high c produces very accurate results. The use of an optimization technique as suggested by Rippa will be the subject of a forthcoming work.

6. Free vibration analysis

Let us assume an harmonic solution for our eigen-problem, involving a spatial (x, y) term and a temporal term ($e^{i\omega t}$), being ω the eigen-frequency,

$$u_0(x, y, t) = U(x, y)\, e^{i\omega t}, \tag{29}$$

$$v_0(x, y, t) = V(x, y)\, e^{i\omega t}, \tag{30}$$

$$w_0(x, y, t) = W(x, y)\, e^{i\omega t}, \tag{31}$$

$$\phi_x(x, y, t) = \Psi_x(x, y)\, e^{i\omega t}, \tag{32}$$

$$\phi_y(x, y, t) = \Psi_y(x, y)\, e^{i\omega t}, \tag{33}$$

$$\phi_x^*(x, y, t) = \Psi_x^*(x, y)\, e^{i\omega t}, \tag{34}$$

$$\phi_x^*(x, y, t) = \Psi_y^*(x, y)\, e^{i\omega t}. \tag{35}$$

Substituting these solutions into the equations of motion, we obtain the equations presented in Appendix B, that represent a generalized eigen-problem, in the form

$$L(U, V, W, \Psi_x, \Psi_y, \Psi_x^*, \Psi_y^*) = \omega^2(U, V, W, \Psi_x, \Psi_y, \Psi_x^*, \Psi_y^*) \tag{36}$$

being L a linear differential operator. We add some boundary conditions to these equations, so our problem can be generically described by

$$L\mathbf{u} + \lambda\mathbf{u} = 0 \text{ in } \Omega, \tag{37}$$

$$B\mathbf{u} = 0 \text{ on } \partial\Omega, \tag{38}$$

where L and B are linear elliptical partial differential operators and Ω a bounded domain in $\mathbb{R}^n$ with some boundary $\partial\Omega$. Following the interpolation method described in Section 5, our global set of equations are now defined as

$$\begin{pmatrix} L_{ii}(g) & L_{ib}(g) \\ B_{bi}(g) & B_{bb}(g) \end{pmatrix} \begin{pmatrix} \alpha_i \\ \alpha_b \end{pmatrix} = \lambda \begin{pmatrix} g_{ii} & g_{ib} \\ \mathbf{0} & \mathbf{0} \end{pmatrix} \begin{pmatrix} \alpha_i \\ \alpha_b \end{pmatrix}. \tag{39}$$

7. Homogenization of material properties

We assume that the plate is composed of two randomly distributed isotropic constituents. We also assume that the macroscopic response of the functionally graded equivalent material is isotropic in the inplane components, and the composition of the composite varies only in the z-direction.

The volume fraction of constituent 2 is given by

$$V_2 = v_2^b + (v_2^t - v_2^b)(0.5 + z/h)^p, \tag{40}$$

where v_2^t and v_2^b are the volume fraction of constituent 2 at the top and bottom of the plate, and $v_2^t = 1; v_2^b = 0$. Factor p controls the content of a constituent as seen in (Fig. 1).

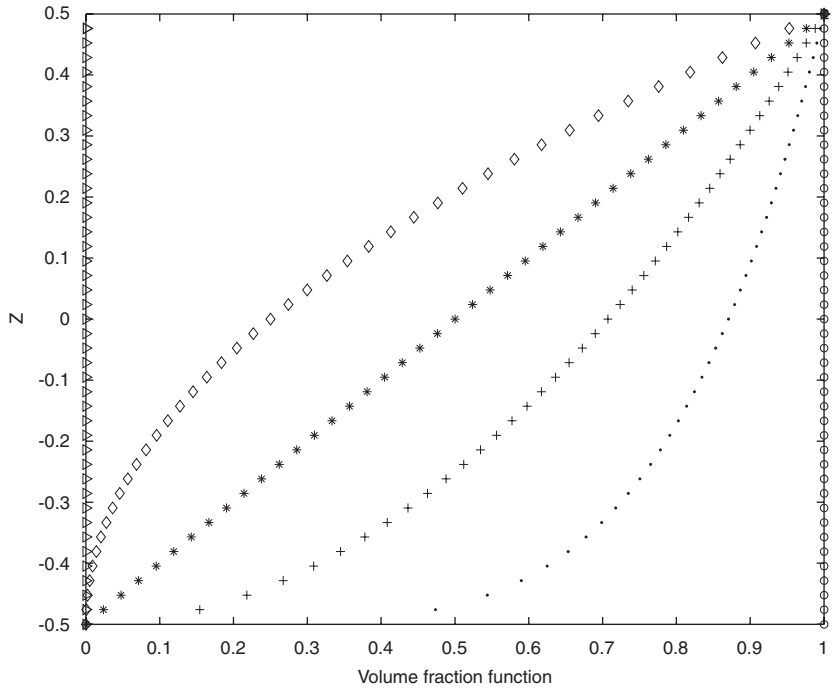

Fig. 1. Influence of factor p in the volume fraction function: $\circ\, p = 0.0; \cdot\, p = 0.2; + p = 0.5; * p = 1.0; \diamond p = 2.0; \triangleright p = 300$.

According to the Mori–Tanaka homogenization method [29] the effective bulk modulus, K, and the effective shear modulus, G, of the composite are given by

$$\frac{K-K_1}{K_2-K_1} = \frac{V_2}{1+(1-V_2)[(K_2-K_1)/(K_1+\frac{4}{3}G_1)]},$$
$$\frac{G-G_1}{G_2-G_1} = \frac{V_2}{1+(1-V_2)[(G_2-G_1)/(G_1+f_1)]}, \tag{41}$$

where

$$f_1 = \frac{G_1(9K_1+8G_1)}{6(K_1+2G_1)}$$

and subscripts 1, 2 refer to constituents 1, 2. The effective values of the Young's modulus, E, and the Poisson's ratio, v, are found from

$$E = \frac{9KG}{3K+G}, \quad v = \frac{3K-2G}{2(3K+G)}. \tag{42}$$

8. Results

We consider three types of boundary conditions, simply supported (S), clamped (C) and free (F). As an example, at a point $a(x,0)$, the boundary conditions are expressed as

$$S: u(a)=0; \quad w(a)=0; \quad \phi_x(a)=0; \quad \phi_x^*(a)=0; \quad N_{yy}(a)=0; \quad M_{yy}(a)=0; \quad S_{yy}(a)=0,$$
$$C: u(a)=0; \quad v(a)=0; \quad w(a)=0; \quad \phi_x(a)=0; \quad \phi_x^*(a)=0; \quad \phi_y(a)=0; \quad \phi_y^*(a)=0,$$
$$F: N_{yy}(a)=0; \quad N_{xy}(a)=0; \quad M_{yy}(a)=0; \quad M_{xy}(a)=0; \quad S_{yy}(a)=0; \quad S_{xy}(a)=0; \quad Q_{yz}(a)=0.$$

The materials of the functionally graded plate, with dimensions $a \times a$, are aluminum and zirconia, with the following material properties:

$$\text{aluminum:} \quad E_a = 70\,\text{GPa}; \quad v_a = 0.3; \quad \rho_a = 2702\,\text{kg/m}^3,$$

$$\text{zirconia:} \quad E_z = 200\,\text{GPa}; \quad v_z = 0.3; \quad \rho_z = 5700\,\text{kg/m}^3. \tag{43}$$

Results are compared with a previous work by the authors [15,30], where the multiquadric method and a third-order plate theory of Reddy are used and the Meshless Local Petrov–Galerkin method (MLPG) is used with a 8×8 nodal arrangement [15]. All frequencies presented in the following tables (Tables 1–7) are non-dimensionalized as follows:

$$\bar{\lambda} = \lambda h \sqrt{\rho / E_{\text{a}}}. \tag{44}$$

In Figs. 2–5 (eig $\equiv \bar{\lambda}$), the contour lines of the flexural vibration modes for different boundary conditions are presented. In Fig. 3 some of the frequencies do not exhibit a flexural mode, so they are plotted as a blank square.

Table 1
Evolution of first 10 natural frequencies ($\bar{\lambda}$) with N, for SSSS plate, $c = 2/\sqrt{N}$, $a/h = 5$, ceramic plate, $p = 1$, $p = 2$, $p = 5$, metal plate

Mode	N					[30] ($N = 11$)	Error w.r.t. [30] (%)
	7	9	11	13	15		
Ceramic							
1	0.2477	0.2466	0.2462	0.2460	0.2459	0.2469	0.4
2	0.4431	0.4487	0.4510	0.4521	0.4526	0.4535	0.2
3	0.4435	0.4488	0.4510	0.4521	0.4526	0.4535	0.2
4	0.5458	0.5408	0.5392	0.5386	0.5383	0.5441	1.1
5	0.5461	0.5409	0.5393	0.5386	0.5384	0.5441	1.0
6	0.6619	0.6502	0.6457	0.6436	0.5815	0.6418	9.4
7	0.7900	0.7828	0.7804	0.7794	0.6426	0.7881	18.5
8	0.8843	0.8980	0.9026	0.9046	0.7789	0.9076	14.2
9	0.8864	0.8985	0.9028	0.9047	0.9056	0.9326	2.9
10	0.9248	0.9197	0.9197	0.9198	0.9056	0.9354	3.2
$p = 1$							
1	0.2199	0.2190	0.2187	0.2186	0.2185	0.2152	1.5
2	0.4022	0.4072	0.4093	0.4103	0.4108	0.4114	0.1
3	0.4026	0.4073	0.4093	0.4103	0.4108	0.4114	0.1
4	0.4863	0.4817	0.4803	0.4797	0.4794	0.4761	0.7
5	0.4865	0.4818	0.4803	0.4797	0.4794	0.4761	0.7
6	0.6005	0.5900	0.5859	0.5840	0.5831	0.5820	0.2
7	0.7049	0.6983	0.6964	0.6953	0.6949	0.6914	0.5
8	0.8023	0.8146	0.8188	0.8206	0.8214	0.8192	0.3
9	0.8041	0.8151	0.8189	0.8206	0.8214	0.8217	3.7×10^{-2}
10	0.8262	0.8213	0.8211	0.8213	0.8215	0.8242	0.3
$p = 2$							
1	0.2205	0.2195	0.2192	0.2191	0.2190	0.2153	1.8
2	0.3945	0.3995	0.4015	0.4024	0.4029	0.4034	0.1
3	0.3949	0.3995	0.4015	0.4025	0.4030	0.4034	0.1
4	0.4835	0.4791	0.4777	0.4772	0.4766	0.4720	1.0
5	0.4837	0.4791	0.4777	0.4772	0.4769	0.4720	1.0
6	0.5890	0.5787	0.5747	0.5729	0.5720	0.5709	0.2
7	0.6976	0.6914	0.6893	0.6885	0.6879	0.6817	1.0
8	0.7870	0.7992	0.8032	0.8050	0.8059	0.8056	3.7×10^{-2}
9	0.7888	0.7996	0.8034	0.8051	0.8059	0.8105	0.6
10	0.8159	0.8114	0.8114	0.8114	0.8114	0.9022	10.1

Table 1 (*continued*)

Mode	N					[30] ($N = 11$)	Error w.r.t. [30] (%)
	7	9	11	13	15		
$p = 5$							
1	0.2232	0.2222	0.2219	0.2217	0.2216	0.2194	1.0
2	0.3876	0.3925	0.3944	0.3954	0.3959	0.3964	0.1
3	0.3879	0.3925	0.3945	0.3954	0.3959	0.3964	0.1
4	0.4848	0.4806	0.4793	0.4787	0.4785	0.4760	0.5
5	0.4850	0.4806	0.4793	0.4787	0.4785	0.4760	0.5
6	0.5788	0.5687	0.5647	0.5629	0.5620	0.5611	0.2
7	0.6961	0.6900	0.6881	0.6872	0.6869	0.6832	0.5
8	0.7734	0.7853	0.7894	0.7911	0.7920	0.7928	0.1
9	0.7752	0.7858	0.7895	0.7911	0.7920	0.8053	1.7
10	0.8119	0.8079	0.8080	0.8081	0.8082	0.8099	0.2
Metal							
1	0.2128	0.2119	0.2116	0.2114	0.2113	0.2122	0.4
2	0.3807	0.3855	0.3875	0.3884	0.3889	0.3897	0.2
3	0.3811	0.3856	0.3875	0.3885	0.3889	0.3897	0.2
4	0.4690	0.4647	0.4633	0.4628	0.4625	0.4675	1.1
5	0.4692	0.4647	0.4634	0.4628	0.4626	0.4675	1.0
6	0.5687	0.5587	0.5548	0.5531	0.5522	0.5517	0.1
7	0.6788	0.6726	0.6706	0.6697	0.6693	0.6772	1.2
8	0.7599	0.7716	0.7756	0.7773	0.7781	0.7615	2.2
9	0.7616	0.7721	0.7757	0.7773	0.7782	0.7799	0.2
10	0.7946	0.7903	0.7903	0.7904	0.7905	0.8013	1.3

Table 2
Evolution of first 10 natural frequencies ($\bar{\lambda}$) with N, for CCCC plate, $c = 2/\sqrt{N}$, $a/h = 5$, ceramic plate, $p = 1$, $p = 2$, $p = 5$, metal plate

Mode	N					[30] ($N = 11$)	Error w.r.t. [30] (%)
	7	9	11	13	15		
Ceramic							
1	0.3816	0.3778	0.3765	0.3762	0.3756	0.3598	4.4
2	0.6647	0.6605	0.6589	0.6582	0.6578	0.6282	4.8
3	0.6647	0.6605	0.6589	0.6584	0.6579	0.6282	4.8
4	0.8729	0.8699	0.8687	0.8682	0.8679	0.8486	2.3
5	0.8729	0.8699	0.8687	0.8682	0.8679	0.8687	0.1
6	0.8986	0.8899	0.8869	0.8856	0.8851	0.8687	1.9
7	0.9983	1.0083	1.0100	1.0101	1.0097	0.9685	4.3
8	1.0127	1.0220	1.0237	1.0242	1.0216	0.9784	4.4
9	1.0313	1.0327	1.0331	1.0333	1.0333	1.0331	1.9×10^{-2}
10	1.2090	1.2029	1.2009	1.1991	1.1987	1.1542	3.9
$p = 1$							
1	0.3405	0.3369	0.3357	0.3352	0.3350	0.3204	4.6
2	0.5948	0.5905	0.5889	0.5883	0.5878	0.5605	4.9
3	0.5948	0.5906	0.5889	0.5884	0.5878	0.5605	4.9
4	0.7905	0.7878	0.7867	0.7862	0.7860	0.7579	3.7
5	0.7905	0.7878	0.7867	0.7862	0.7860	0.7867	0.1
6	0.8050	0.7966	0.7936	0.7916	0.7915	0.7867	0.6
7	0.8948	0.9033	0.9044	0.9040	0.9040	0.8653	4.5
8	0.9076	0.9154	0.9167	0.9167	0.9164	0.8742	4.8
9	0.9353	0.9366	0.9369	0.9371	0.9371	0.9369	2.1×10^{-2}
10	1.0845	1.0783	1.0761	1.0747	1.0741	1.0320	4.1

Table 2 (*continued*)

Mode	N					[30] ($N = 11$)	Error w.r.t. [30] (%)
	7	9	11	13	15		
$p = 2$							
1	0.3379	0.3343	0.3330	0.3325	0.3322	0.3165	5.0
2	0.5870	0.5827	0.5810	0.5799	0.5790	0.5507	5.1
3	0.5871	0.5827	0.5812	0.5803	0.5801	0.5507	5.3
4	0.7757	0.7730	0.7719	0.7715	0.7712	0.7435	3.7
5	0.7757	0.7730	0.7719	0.7715	0.7712	0.7719	0.1
6	0.7928	0.7843	0.7818	0.7798	0.7793	0.7719	1.0
7	0.8809	0.8885	0.8893	0.8889	0.8882	0.8480	4.7
8	0.8933	0.9002	0.9011	0.9009	0.9003	0.8562	5.2
9	0.9176	0.9188	0.9192	0.9193	0.9194	0.9192	2.1×10^{-2}
10	1.0660	1.0593	1.0568	1.0540	1.0545	1.0106	4.3
$p = 5$							
1	0.3381	0.3345	0.3333	0.3327	0.3324	0.3154	5.4
2	0.5836	0.5793	0.5775	0.5763	0.5766	0.5458	5.6
3	0.5836	0.5793	0.5776	0.5767	0.5768	0.5458	5.7
4	0.7626	0.7600	0.7590	0.7585	0.7583	0.7358	3.1
5	0.7626	0.7600	0.7590	0.7585	0.7583	0.7590	0.1
6	0.7862	0.7778	0.7747	0.7737	0.7728	0.7590	1.8
7	0.8729	0.8800	0.8806	0.8799	0.8800	0.8384	5.0
8	0.8851	0.8916	0.8922	0.8919	0.8919	0.8458	5.4
9	0.9018	0.9031	0.9034	0.9035	0.9036	0.9034	2.2×10^{-2}
10	1.0545	1.0477	1.0450	1.0437	1.0420	0.9980	4.4
Metal							
1	0.3279	0.3246	0.3235	0.3232	0.3229	0.3092	4.3
2	0.5711	0.5675	0.5662	0.5658	0.5653	0.5398	4.7
3	0.5711	0.5675	0.5663	0.5737	0.5658	0.5398	4.8
4	0.7501	0.7474	0.7464	0.7460	0.7458	0.7291	2.3
5	0.7501	0.7474	0.7464	0.7460	0.7458	0.7464	0.1
6	0.7721	0.7647	0.7620	0.7610	0.7608	0.7464	1.9
7	0.8578	0.8664	0.8679	0.8667	0.8676	0.8322	4.3
8	0.8702	0.8781	0.8796	0.8807	0.8801	0.8407	4.7
9	0.8862	0.8874	0.8877	0.8879	0.8879	0.8877	2.3×10^{-2}
10	1.0388	1.0336	1.0320	1.0173	1.0304	0.9918	3.9

Table 3
Evolution of first 10 natural frequencies ($\bar{\lambda}$) with N, for FGM CSCS plate, $c = 3/(N-1)$, $a/h = 5$, ceramic plate, $p = 1$, $p = 2$, $p = 5$, metal plate

Mode	N							[30] ($N = 11$)	Error w.r.t. [30] (%)
	9	11	13	15	17	19	21		
Ceramic									
1	0.3193	0.3179	0.3172	0.3168	0.3165	0.3164	0.3163	0.3066	3.2
2	0.4279	0.4314	0.4339	0.4357	0.4372	0.4383	0.4393	0.4509	2.3
3	0.5757	0.5716	0.5694	0.5680	0.5671	0.5665	0.5660	0.5578	1.5
4	0.6382	0.6361	0.6349	0.6343	0.6339	0.6336	0.6334	0.6082	4.1
5	0.7950	0.7943	0.7940	0.7940	0.7940	0.7941	0.7942	0.7997	0.7
6	0.8431	0.8383	0.8357	0.8341	0.8331	0.8324	0.8319	0.8126	2.4
7	0.8624	0.8579	0.8555	0.8540	0.8530	0.8523	0.8518	0.8558	0.5
8	0.8737	0.8790	0.8823	0.8846	0.8863	0.8877	0.8888	0.9025	1.5
9	0.9539	0.9464	0.9424	0.9400	0.9383	0.9371	0.9362	0.9258	1.1
10	1.0089	1.0079	1.0071	1.0065	1.0060	1.0057	1.0055	0.9656	4.1

Table 3 (*continued*)

Mode	N							[30] ($N = 11$)	Error w.r.t. [30] (%)
	9	11	13	15	17	19	21		
$p = 1$									
1	0.2845	0.2832	0.2825	0.2822	0.2819	0.2818	0.2817	0.2729	3.2
2	0.3885	0.3916	0.3939	0.3956	0.3969	0.3979	0.3987	0.4093	2.6
3	0.5133	0.5096	0.5076	0.5064	0.5056	0.5050	0.5045	0.4970	1.5
4	0.5705	0.5684	0.5674	0.5667	0.5663	0.5660	0.5658	0.5426	4.3
5	0.7209	0.7202	0.7100	0.7199	0.7200	0.7200	0.7201	0.7250	0.7
6	0.7537	0.7493	0.7469	0.7454	0.7444	0.7438	0.7433	0.7254	2.5
7	0.7810	0.7770	0.7748	0.7735	0.7726	0.7720	0.7715	0.7750	0.5
8	0.7927	0.7975	0.8005	0.8026	0.8041	0.8054	0.8064	0.8187	1.5
9	0.8524	0.8455	0.8418	0.8396	0.8381	0.8370	0.8361	0.8266	1.1
10	0.9039	0.9027	0.9018	0.9012	0.9007	0.9004	0.9001	0.8629	4.3
$p = 2$									
1	0.2829	0.2816	0.2810	0.2806	0.2804	0.2802	0.2801	0.2706	3.5
2	0.3810	0.3841	0.3863	0.3880	0.3893	0.3903	0.3911	0.4014	2.6
3	0.5093	0.5057	0.5037	0.5025	0.5017	0.5011	0.5007	0.4928	1.6
4	0.5633	0.5612	0.5601	0.5594	0.5590	0.5587	0.5585	0.5340	4.6
5	0.7072	0.7065	0.7063	0.7063	0.7063	0.7064	0.7065	0.7113	0.7
6	0.7438	0.7394	0.7370	0.7355	0.7345	0.7339	0.7334	0.7147	2.7
7	0.7664	0.7624	0.7603	0.7589	0.7581	0.7575	0.7570	0.7604	0.4
8	0.7777	0.7823	0.7853	0.7873	0.7889	0.7901	0.7911	0.8032	1.5
9	0.8411	0.8344	0.8309	0.8288	0.8273	0.8262	0.8254	0.8158	1.2
10	0.8891	0.8877	0.8867	0.8859	0.8854	0.8850	0.8847	0.8460	4.6
$p = 5$									
1	0.2839	0.2826	0.2819	0.2815	0.2813	0.2811	0.2810	0.2709	3.7
2	0.3743	0.3774	0.3795	0.3812	0.3824	0.3834	0.3842	0.3944	2.6
3	0.5096	0.5060	0.5041	0.5029	0.5021	0.5015	0.5011	0.4930	1.6
4	0.5605	0.5584	0.5572	0.5565	0.5561	0.5558	0.5556	0.5302	4.8
5	0.6951	0.6944	0.6942	0.6942	0.6942	0.6943	0.6944	0.6991	0.7
6	0.7396	0.7352	0.7328	0.7314	0.7304	0.7298	0.7293	0.7101	2.7
7	0.7535	0.7496	0.7475	0.7462	0.7453	0.7447	0.7443	0.7477	0.5
8	0.7642	0.7688	0.7716	0.7737	0.7752	0.7764	0.7774	0.7893	1.5
9	0.8363	0.8299	0.8266	0.8245	0.8231	0.8221	0.8213	0.8116	1.2
10	0.8806	0.8792	0.8780	0.8773	0.8767	0.8763	0.8760	0.8366	4.7
Metal									
1	0.2744	0.2732	0.2725	0.2722	0.2720	0.2718	0.2718	0.2635	3.1
2	0.3677	0.3707	0.3728	0.3744	0.3757	0.3766	0.3775	0.3875	2.6
3	0.4947	0.4912	0.4893	0.4881	0.4873	0.4867	0.4863	0.4793	1.5
4	0.5484	0.5466	0.5456	0.5450	0.5446	0.5444	0.5442	0.5226	4.1
5	0.6832	0.6825	0.6823	0.6823	0.6823	0.6824	0.6825	0.6871	0.7
6	0.7245	0.7203	0.7181	0.7167	0.7158	0.7152	0.7148	0.6982	2.4
7	0.7410	0.7372	0.7351	0.7338	0.7330	0.7324	0.7320	0.7354	0.5
8	0.7507	0.7553	0.7581	0.7601	0.7616	0.7628	0.7638	0.7755	1.5
9	0.8197	0.8132	0.8098	0.8077	0.8062	0.8052	0.8044	0.7955	1.1
10	0.8669	0.8661	0.8654	0.8648	0.8645	0.8642	0.8640	0.8297	4.1

In general, the relative error is small, decreasing with the number of points/side. In some cases, the error does not follow this tendency, which is a problem previously found by the authors and others. It is well known that the multiquadric method produces ill-conditioned matrices, a problem that increases with the number of mesh points (N is the number of points per side). Some authors reduce the conditioning number by using pre-conditioners [22].

In Table 5 the evolution of non-dimensional frequency ($\bar{\lambda}$) with the number of nodes, for a/h ratios of a simply supported plate, is compared with exact results of Vel and Batra [31]. The error is below 1% for all

Table 4
Evolution of first 10 natural frequencies ($\bar{\lambda}$) with N, for FGM CFCF plate, $c = 3/(N-1)$, $a/h = 5$, ceramic plate, $p = 1$, $p = 2$, $p = 5$, metal plate

Mode	N							[30] ($N = 11$)	Error w.r.t. [30] (%)
	7	9	11	13	15	17	19		
Ceramic									
1	0.2619	0.1875	0.1899	0.2000	0.2088	0.2159	0.2215	0.2362	6.2
2	0.3745	0.2105	0.2083	0.2120	0.2159	0.2192	0.2218	0.2614	15.1
3	0.3763	0.3784	0.3823	0.3866	0.3906	0.3941	0.3970	0.4227	6.1
4	0.3903	0.4007	0.4025	0.4031	0.4034	0.4036	0.4038	0.4248	4.9
5	0.3945	0.4369	0.4707	0.4914	0.5049	0.5141	0.5207	0.5310	1.9
6	0.4880	0.4375	0.4739	0.4976	0.5137	0.5252	0.5338	0.5669	5.8
7	0.4880	0.6858	0.6867	0.6902	0.6942	0.6979	0.7012	0.7298	3.9
8	0.6946	0.7423	0.7363	0.7331	0.7318	0.7314	0.7314	0.7417	1.4
9	0.7318	0.7446	0.7422	0.7405	0.7393	0.7384	0.7377	0.7469	1.2
10	0.7455	0.7446	0.7467	0.7489	0.7503	0.7512	0.7519	0.7521	2.7×10^{-2}
$p = 1$									
1	0.2456	0.1652	0.1652	0.1745	0.1828	0.1894	0.1947	0.2117	8.0
2	0.3230	0.1867	0.1833	0.1867	0.1904	0.1935	0.1960	0.2324	15.7
3	0.3357	0.3356	0.3388	0.3426	0.3463	0.3494	0.3521	0.3769	6.6
4	0.3372	0.3634	0.3651	0.3657	0.3660	0.3662	0.3664	0.3834	4.4
5	0.3576	0.3816	0.4143	0.4344	0.4475	0.4563	0.4627	0.4734	2.3
6	0.4106	0.3819	0.4167	0.4392	0.4545	0.4655	0.4737	0.5056	6.3
7	0.4106	0.6110	0.6117	0.6149	0.6184	0.6218	0.6249	0.6507	4.0
8	0.6191	0.6639	0.6560	0.6531	0.6520	0.6517	0.6518	0.6612	1.4
9	0.6626	0.6724	0.6723	0.6708	0.6697	0.6690	0.6684	0.6766	1.2
10	0.6768	0.6744	0.6764	0.6785	0.6798	0.6807	0.6813	0.6816	4.4×10^{-2}
$p = 2$									
1	0.2377	0.1683	0.1686	0.1771	0.1847	0.1908	0.1958	0.2089	6.3
2	0.3272	0.1882	0.1851	0.1881	0.1913	0.1942	0.1964	0.2298	14.5
3	0.3390	0.3364	0.3392	0.3429	0.3463	0.3493	0.3519	0.3755	6.3
4	0.3393	0.3565	0.3581	0.3587	0.3590	0.3592	0.3594	0.3761	4.4
5	0.3508	0.3823	0.4127	0.4316	0.4438	0.4522	0.4581	0.4654	1.6
6	0.4315	0.3825	0.4156	0.4369	0.4514	0.4618	0.4695	0.4981	5.7
7	0.4315	0.6048	0.6055	0.6085	0.6120	0.6153	0.6182	0.6425	3.8
8	0.6130	0.6594	0.6516	0.6487	0.6475	0.6472	0.6472	0.6566	1.4
9	0.6502	0.6597	0.6596	0.6582	0.6571	0.6563	0.6558	0.6639	1.2
10	0.6644	0.6617	0.6637	0.6658	0.6670	0.6679	0.6685	0.6687	3.0×10^{-2}
$p = 5$									
1	0.2293	0.1732	0.1744	0.1822	0.1893	0.1950	0.1992	0.2103	5.3
2	0.3381	0.1913	0.1891	0.1917	0.1946	0.1971	0.1995	0.2306	13.5
3	0.3424	0.3404	0.3432	0.3467	0.3499	0.3527	0.3531	0.3696	4.5
4	0.3447	0.3504	0.3519	0.3525	0.3527	0.3529	0.3552	0.3764	5.6
5	0.3497	0.3891	0.4167	0.4340	0.4452	0.4527	0.4582	0.4617	0.8
6	0.3782	0.3896	0.4204	0.4402	0.4536	0.4633	0.4706	0.4952	5.0
7	0.5247	0.6039	0.6046	0.6076	0.6110	0.6142	0.6170	0.6398	3.6
8	0.6120	0.6486	0.6485	0.6470	0.6460	0.6452	0.6447	0.6527	1.2
9	0.6393	0.6506	0.6524	0.6494	0.6482	0.6479	0.6478	0.6570	1.4
10	0.6532	0.6600	0.6525	0.6545	0.6557	0.6565	0.6571	0.6574	4.6×10^{-2}
Metal									
1	0.2250	0.1611	0.1632	0.1718	0.1794	0.1855	0.1903	0.2044	6.9
2	0.3218	0.1809	0.1790	0.1822	0.1855	0.1883	0.1906	0.2250	15.3
3	0.3235	0.3252	0.3285	0.3323	0.3357	0.3386	0.3412	0.3632	6.1
4	0.3354	0.3444	0.3458	0.3464	0.3466	0.3468	0.3470	0.3657	5.1
5	0.3389	0.3754	0.4045	0.4223	0.4338	0.4417	0.4474	0.4563	2.0
6	0.4185	0.3759	0.4072	0.4275	0.4413	0.4512	0.4587	0.4871	5.9

Table 4 (*continued*)

Mode	N							[30] ($N = 11$)	Error w.r.t. [30] (%)
	7	9	11	13	15	17	19		
7	0.4185	0.5893	0.5901	0.5931	0.5965	0.5997	0.6025	0.6270	4.0
8	0.5968	0.6378	0.6327	0.6299	0.6288	0.6285	0.6285	0.6374	1.4
9	0.6288	0.6398	0.6377	0.6363	0.6352	0.6345	0.6339	0.6418	1.2
10	0.6425	0.6399	0.6416	0.6435	0.6447	0.6455	0.6460	0.6463	4.6×10^{-2}

Table 5
Evolution of fundamental frequency, $\bar{\lambda}$ with N, for various a/h ratios for SSSS plate, $p = 1$, $c = 2/\sqrt{N}$

Grid	a/h		
	5	10	20
7×7	0.2199	0.0588	0.0140
9×7	0.2190	0.0593	0.0148
11×7	0.2187	0.0595	0.0152
13×7	0.2186	0.0595	0.0156
15×7	0.2185	0.0595	0.0152
17×7	0.2184	0.0595	0.0152
19×7	0.2184	0.0589	0.0152
exact [31]	0.2192	0.0596	0.0153
error (%)	0.4	1.2	0.7

Table 6
Evolution of fundamental frequency, $\bar{\lambda}$ with N, for various factors p for SSSS plate, $a/h = 5$, $c = 2/\sqrt{N}$

Grid	p		
	2	3	5
7×7	0.2205	0.2219	0.2232
9×7	0.2195	0.2209	0.2222
11×7	0.2192	0.2206	0.2219
13×7	0.2191	0.2204	0.2217
15×7	0.2190	0.2204	0.2216
17×7	0.2190	0.2203	0.2216
19×7	0.2189	0.2203	0.2216
exact [31]	0.2197	0.2211	0.2225
error (%)	0.4	0.4	0.4

cases. The exponent p is set to 1 and we use a shape parameter $c = 2/\sqrt{N}$, where N is the number of nodes per side in a regular grid.

In Table 6 the non-dimensional frequency is compared with exact results of Vel and Batra. Here, we vary the number of nodes in a regular grid and we consider various exponents p. The plate is rather thick with a side/thickness ratio a/h set as 5. Errors remain as small as 0.4%.

Due to lack of published results in the literature for various boundary conditions, we compare the present solution with previous results by the authors [30], using a higher-order theory of Reddy [32]. In Table 7 we consider a simply supported plate with $p = 1$. We consider two a/h ratios and the first 10 frequencies are listed. It can be seen that the present model and the model used on Reddy's theory show very close agreement.

For various values of p, with $a/h = 5$, a simply supported functionally graded plate is considered in Table 1. The first 10 natural frequencies are listed for various grids. Results are compared with those of Ref. [30]. Again the present method shows similar results.

Table 7
Evolution of first 10 natural frequencies ($\bar{\lambda}$) with N, for SSSS plate, $a/h = 10, 20$, $c = 2/\sqrt{N}$, $p = 1$

Mode	N						[30] ($N = 11$)	Error w.r.t. [30] (%)
	7	9	11	13	15	17		
$a/h = 10$								
1	0.0588	0.0593	0.0595	0.0595	0.0595	0.0595	0.0584	1.9
2	0.1463	0.1435	0.1427	0.1423	0.1423	0.1421	0.1410	0.8
3	0.1464	0.1436	0.1429	0.1425	0.1426	0.1422	0.1410	0.9
4	0.2011	0.2036	0.2047	0.2052	0.2054	0.2056	0.2058	0.1
5	0.2013	0.2037	0.2047	0.2052	0.2054	0.2056	0.2058	0.1
6	0.2230	0.2201	0.2194	0.2187	0.2186	0.2185	0.2164	1.0
7	0.2739	0.2681	0.2670	0.2663	0.2656	0.2663	0.2646	0.6
8	0.2745	0.2682	0.2672	0.2667	0.2664	0.2663	0.2677	0.5
9	0.3003	0.2951	0.2930	0.2921	0.2916	0.2914	0.2913	3.4×10^{-2}
10	0.3465	0.3380	0.3356	0.3350	0.3344	0.3343	0.3264	2.4
$a/h = 20$								
1	0.0140	0.0148	0.0152	0.0156	0.0152	0.0152	0.0149	2.0
2	0.0391	0.0381	0.0374	0.0378	0.0377	0.0377	0.0377	0.0
3	0.0392	0.0382	0.0378	0.0378	0.0377	0.0378	0.0377	0.3
4	0.0604	0.0595	0.0598	0.0596	0.0595	0.0595	0.0593	0.3
5	0.0807	0.0757	0.0746	0.0742	0.0739	0.0739	0.0747	1.1
6	0.0812	0.0760	0.0757	0.0772	0.0740	0.0739	0.0747	1.1
7	0.1000	0.0963	0.0951	0.0952	0.0949	0.0950	0.0769	23.5
8	0.1006	0.0970	0.0957	0.0957	0.0951	0.0950	0.0912	4.2
9	0.1007	0.1018	0.1023	0.1026	0.1027	0.1028	0.0913	12.6
10	0.1023	0.1019	0.1024	0.1026	0.1027	0.1028	0.1029	0.1

In Table 2 we present the same problem of Table 1, with the exception of considering a fully clamped plate. Frequencies of the present model are slightly higher than the model presented in Ref. [30].

For a CSCS (clamped/simply supported/clamped/simply supported) plate we show the first 10 natural frequencies in Table 3. The model shows again slightly higher frequencies than in Ref. [30].

In Table 4 we consider a CFCF (clamped/free/clamped/free) plate. Results for the first 10 natural frequencies are very similar to those of Ref. [30].

9. Concluding remarks

In this paper, we used the multiquadric radial basis function method to obtain natural frequencies of functionally graded plates.

The use of multiquadrics provides an adequate framework for the free vibration analysis of functionally graded plates. The choice of the shape parameter by the user is a typical drawback of the method, to be solved in the future by an optimization technique.

We used a third-order formulation based on the work of Kant and colleagues. The equations of motion are discretized into a generalized eigenvalue/eigenvector problem and solved by Matlab.

Various functionally graded materials are considered. Also several boundary conditions are proposed. Results are compared with those of Batra and colleagues who used an alternative meshless method and with exact formulations. We tested various side-to-thickness ratios, with fully simply supported or fully clamped boundary conditions. Also, various exponents p were used, to test various material possibilities.

The homogeneization technique is the Mori–Tanaka scheme, that is accepted today as one of the best approximation for the equivalent isotropic material properties of the graded composite. All stiffness components are evaluated by symbolic integration with MATLAB.

Present results show that this meshless method is a reliable alternative to finite element methods, regardless the variation of plate thickness and ceramic/metal contents.

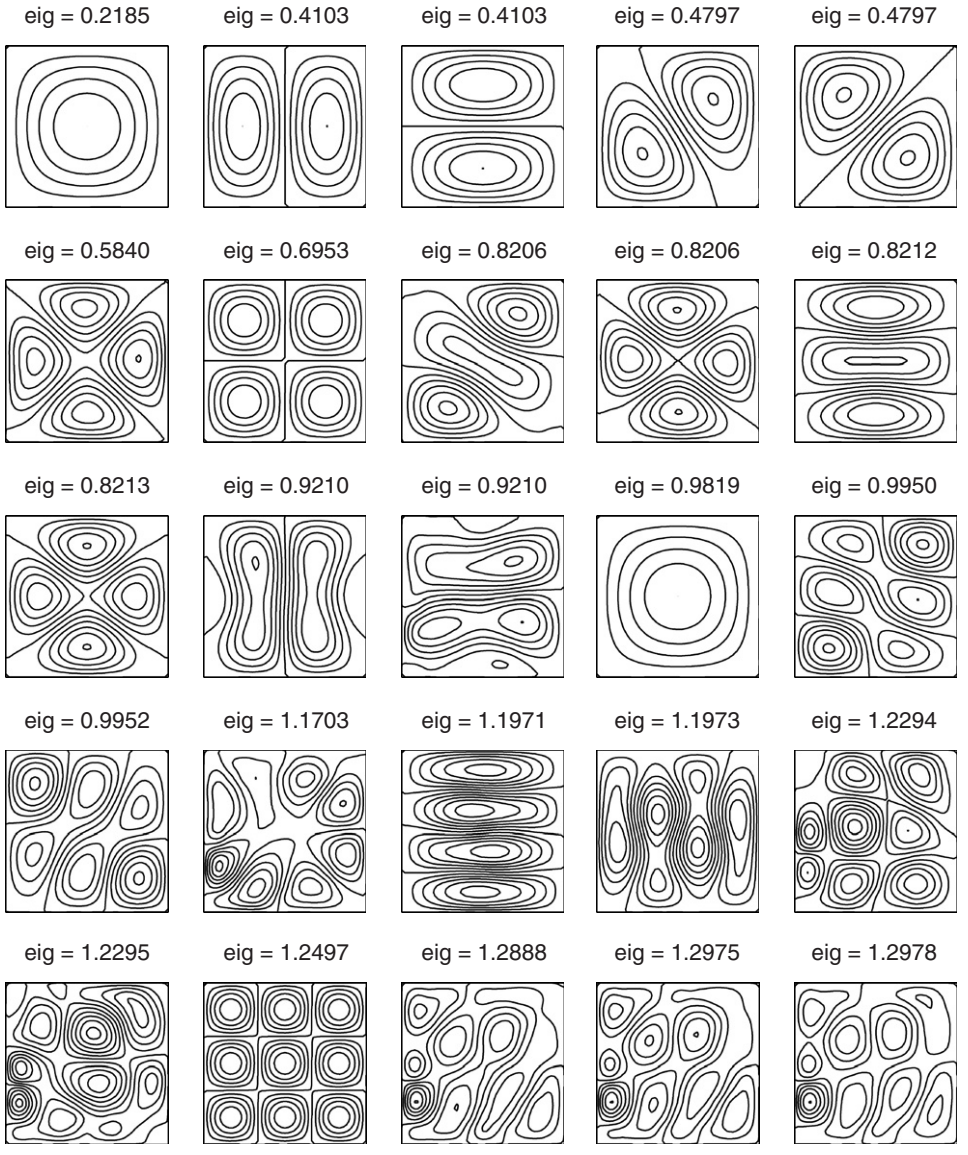

Fig. 2. Evolution of first 25 flexural modes, for FGM SSSS plate, $a/h = 5$, $c = 2/\sqrt{N}$, $p = 1$, $N = 13$.

Appendix A

The Euler–Lagrange equations written in terms of the displacements are expressed by

$$
\begin{aligned}
&-A_{11}\frac{\partial^2 u_0}{\partial x^2}-A_{12}\frac{\partial^2 v_0}{\partial x\partial y}-A_{13}\left(2\frac{\partial^2 u_0}{\partial x\partial y}+\frac{\partial^2 v_0}{\partial x^2}\right)-A_{23}\frac{\partial^2 v_0}{\partial y^2}-A_{33}\left(\frac{\partial^2 u_0}{\partial y^2}+\frac{\partial^2 v_0}{\partial x\partial y}\right)\\
&-B_{11}\frac{\partial^2 \phi_x}{\partial x^2}-B_{12}\frac{\partial^2 \phi_y}{\partial x\partial y}-B_{13}\left(2\frac{\partial^2 \phi_x}{\partial x\partial y}+\frac{\partial^2 \phi_y}{\partial x^2}\right)-B_{23}\frac{\partial^2 \phi_y}{\partial y^2}-B_{33}\left(\frac{\partial^2 \phi_x}{\partial y^2}+\frac{\partial^2 \phi_y}{\partial x\partial y}\right)\\
&-E_{11}\frac{\partial^2 \phi_x^*}{\partial x^2}-E_{12}\frac{\partial^2 \phi_y^*}{\partial x\partial y}-E_{13}\left(2\frac{\partial^2 \phi_x^*}{\partial x\partial y}+\frac{\partial^2 \phi_y^*}{\partial x^2}\right)-E_{23}\frac{\partial^2 \phi_y^*}{\partial y^2}-E_{33}\left(\frac{\partial^2 \phi_x^*}{\partial y^2}+\frac{\partial^2 \phi_y^*}{\partial x\partial y}\right)\\
&=I_0\ddot{u}_0+I_1\ddot{\phi}_x+I_3\ddot{\phi}_x^*,
\end{aligned}
\tag{45a}
$$

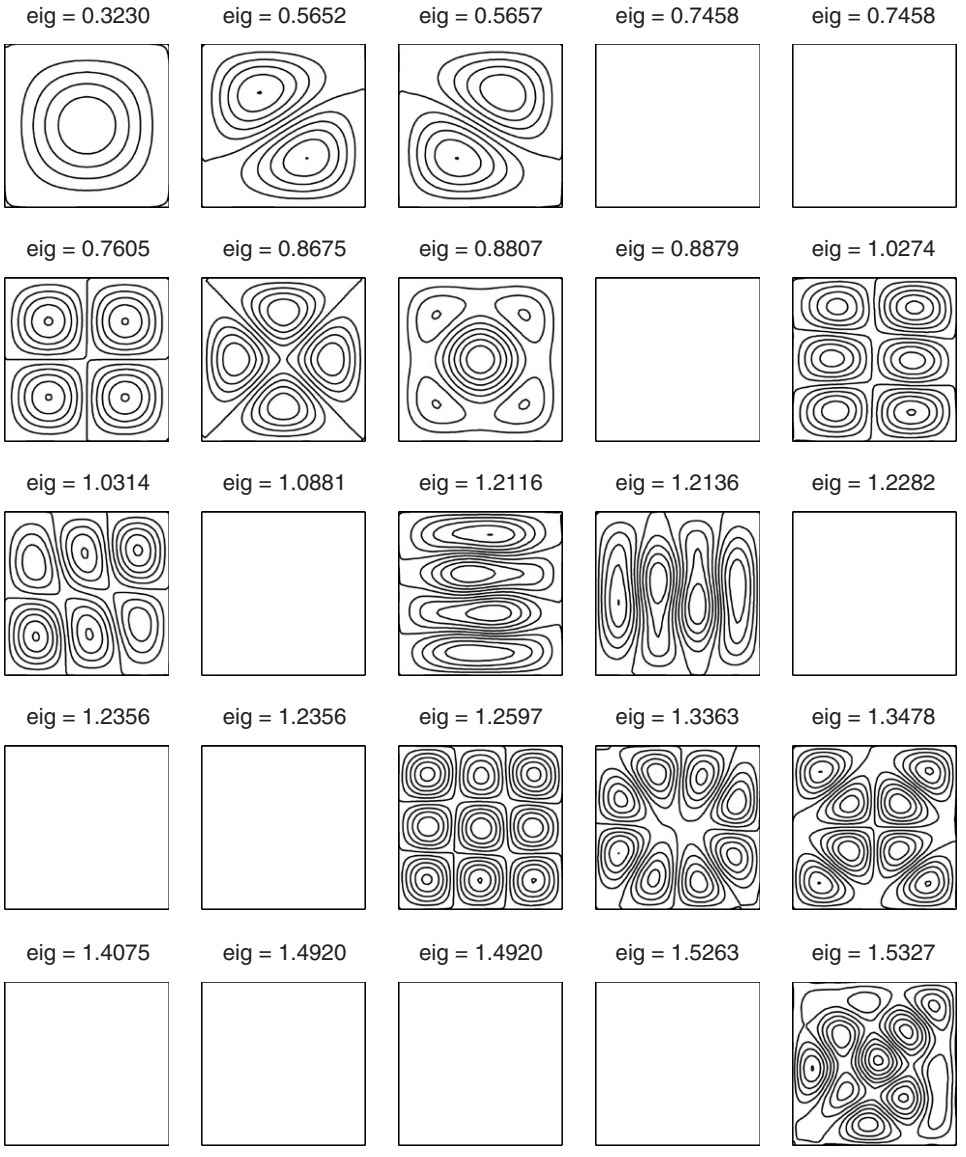

Fig. 3. Evolution of first 25 flexural modes, for FGM CCCC plate, $a/h = 5$, $c = 2/\sqrt{N}$, metal plate, $N = 15$.

$$
\begin{aligned}
&- A_{12}\frac{\partial^2 u_0}{\partial x \partial y} - A_{22}\frac{\partial^2 v_0}{\partial y^2} - A_{23}\left(\frac{\partial^2 u_0}{\partial y^2} + 2\frac{\partial^2 v_0}{\partial x \partial y}\right) - A_{13}\frac{\partial^2 u_0}{\partial x^2} - A_{33}\left(\frac{\partial^2 u_0}{\partial x \partial y} + \frac{\partial^2 v_0}{\partial x^2}\right)\\
&- B_{12}\frac{\partial^2 \phi_x}{\partial x \partial y} - B_{22}\frac{\partial^2 \phi_y}{\partial y^2} - B_{23}\left(\frac{\partial^2 \phi_x}{\partial y^2} + 2\frac{\partial^2 \phi_y}{\partial x \partial y}\right) - B_{13}\frac{\partial^2 \phi_x}{\partial x^2} - B_{33}\left(\frac{\partial^2 \phi_x}{\partial x \partial y} + \frac{\partial^2 \phi_y}{\partial x^2}\right)\\
&- E_{12}\frac{\partial^2 \phi_x^*}{\partial x \partial y} - E_{22}\frac{\partial^2 \phi_y^*}{\partial y^2} - E_{23}\left(\frac{\partial^2 \phi_x^*}{\partial y^2} + 2\frac{\partial^2 \phi_y^*}{\partial x \partial y}\right) - E_{13}\frac{\partial^2 \phi_x^*}{\partial x^2} - E_{33}\left(\frac{\partial^2 \phi_x^*}{\partial x \partial y} + \frac{\partial^2 \phi_y^*}{\partial x^2}\right)\\
&= I_0\ddot{v}_0 + I_1\ddot{\phi}_y + I_3\ddot{\phi}_y^*, \qquad (45b)
\end{aligned}
$$

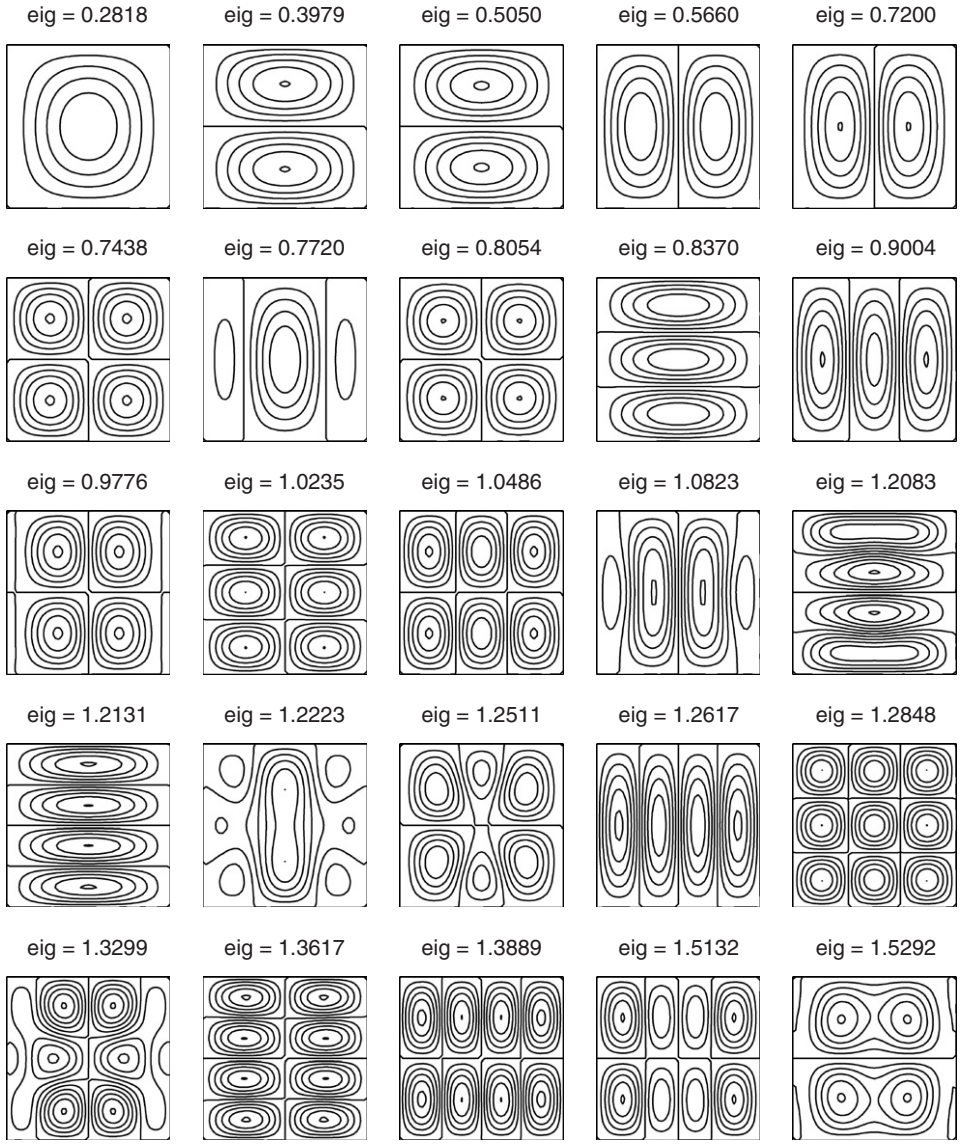

Fig. 4. Evolution of first 25 flexural modes, for FGM CSCS plate, $a/h = 5$, $c = 3/(N-1)$, $p = 1$, $N = 19$.

$$- I_{44}\left(\frac{\partial \phi_y}{\partial y} + \frac{\partial^2 w_0}{\partial y^2}\right) - I_{45}\left(\frac{\partial \phi_x}{\partial y} + 2\frac{\partial^2 w_0}{\partial x \partial y} + \frac{\partial \phi_y}{\partial x}\right) - I_{55}\left(\frac{\partial \phi_x}{\partial x} + \frac{\partial^2 w_0}{\partial x^2}\right)$$
$$- 3K_{44}\frac{\partial \phi_y^*}{\partial y} - 3K_{45}\left(\frac{\partial \phi_x^*}{\partial y} + \frac{\partial \phi_y^*}{\partial x}\right) - 3K_{55}\frac{\partial \phi_x^*}{\partial x} - q = I_0 \ddot{w}_0, \tag{45c}$$

$$- B_{11}\frac{\partial^2 u_0}{\partial x^2} - B_{12}\frac{\partial^2 v_0}{\partial x \partial y} - B_{13}\left(2\frac{\partial^2 u_0}{\partial x \partial y} + \frac{\partial^2 v_0}{\partial x^2}\right) - B_{23}\frac{\partial^2 v_0}{\partial y^2} - B_{33}\left(\frac{\partial^2 u_0}{\partial y^2} + \frac{\partial^2 v_0}{\partial x \partial y}\right)$$
$$- F_{11}\frac{\partial^2 \phi_x}{\partial x^2} - F_{12}\frac{\partial^2 \phi_y}{\partial x \partial y} - F_{13}\left(2\frac{\partial^2 \phi_x}{\partial x \partial y} + \frac{\partial^2 \phi_y}{\partial x^2}\right) - F_{23}\frac{\partial^2 \phi_y}{\partial y^2} - F_{33}\left(\frac{\partial^2 \phi_x}{\partial y^2} + \frac{\partial^2 \phi_y}{\partial x \partial y}\right)$$

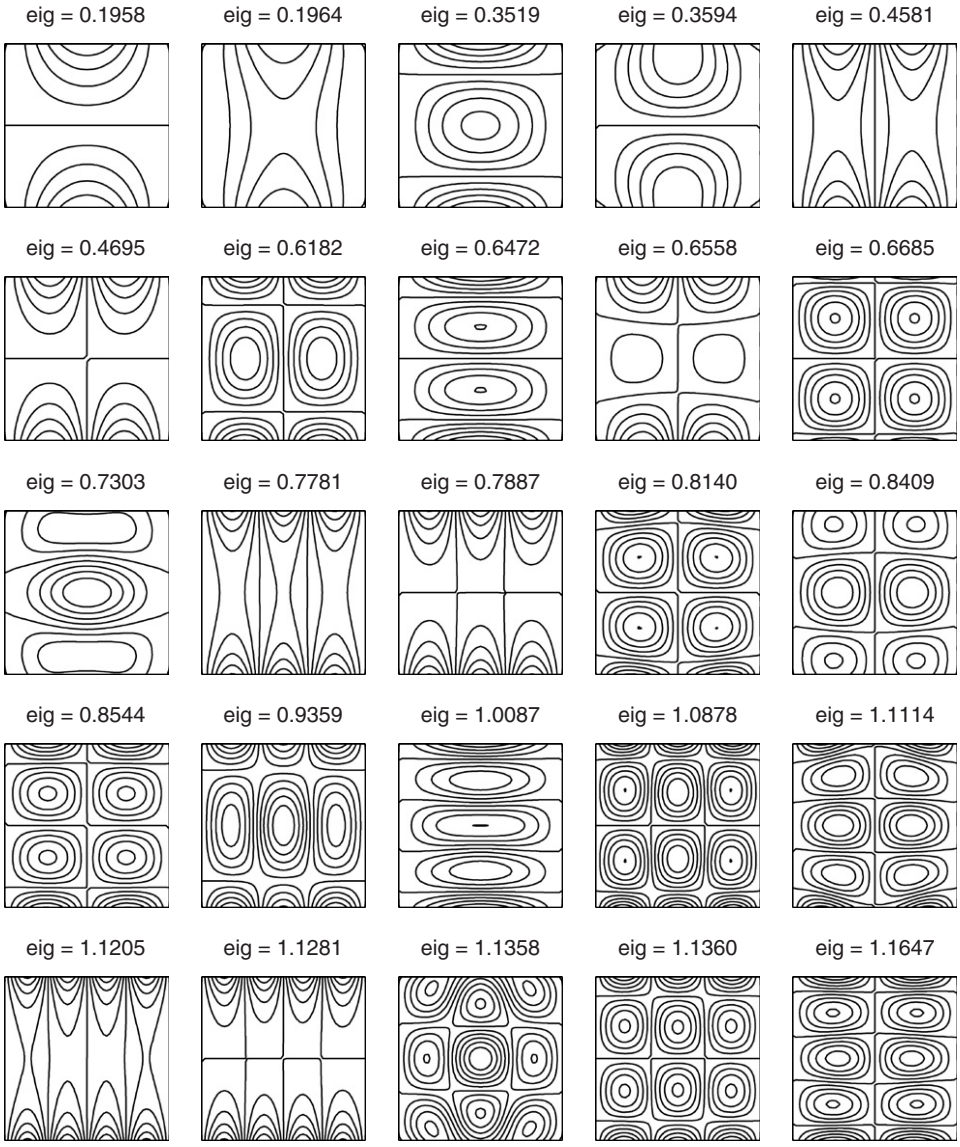

Fig. 5. Evolution of first 25 flexural modes, for FGM CFCF plate, $a/h = 5$, $c = 3/(N-1)$, $p = 2$, $N = 19$.

$$- G_{11}\frac{\partial^2\phi_x^*}{\partial x^2} - G_{12}\frac{\partial^2\phi_y^*}{\partial x\partial y} - G_{13}\left(2\frac{\partial^2\phi_x^*}{\partial x\partial y} + \frac{\partial^2\phi_y^*}{\partial x^2}\right) - G_{23}\frac{\partial^2\phi_y^*}{\partial y^2} - G_{33}\left(\frac{\partial^2\phi_x^*}{\partial y^2} + \frac{\partial^2\phi_y^*}{\partial x\partial y}\right)$$
$$+ I_{45}\left(\phi_y + \frac{\partial w_0}{\partial y}\right) + I_{55}\left(\phi_x + \frac{\partial w_0}{\partial x}\right) + 3K_{45}\phi_y^* + 3K_{55}\phi_x^* = I_1\ddot{u}_0 + I_2\ddot{\phi}_x + I_4\ddot{\phi}_x^*, \tag{45d}$$
$$- B_{12}\frac{\partial^2 u_0}{\partial x\partial y} - B_{22}\frac{\partial^2 v_0}{\partial y^2} - B_{23}\left(\frac{\partial^2 u_0}{\partial y^2} + 2\frac{\partial^2 v_0}{\partial x\partial y}\right) - B_{13}\frac{\partial^2 u_0}{\partial x^2} - B_{33}\left(\frac{\partial^2 u_0}{\partial x\partial y} + \frac{\partial^2 v_0}{\partial x^2}\right)$$
$$- F_{12}\frac{\partial^2\phi_x}{\partial x\partial y} - F_{22}\frac{\partial^2\phi_y}{\partial y^2} - F_{23}\left(\frac{\partial^2\phi_x}{\partial y^2} + 2\frac{\partial^2\phi_y}{\partial x\partial y}\right) - F_{13}\frac{\partial^2\phi_x}{\partial x^2} - F_{33}\left(\frac{\partial^2\phi_x}{\partial x\partial y} + \frac{\partial^2\phi_y}{\partial x^2}\right)$$

$$
\begin{aligned}
&- G_{12}\frac{\partial^2\phi_x^*}{\partial x\partial y} - G_{22}\frac{\partial^2\phi_y^*}{\partial y^2} - G_{23}\left(\frac{\partial^2\phi_x^*}{\partial y^2} + 2\frac{\partial^2\phi_y^*}{\partial x\partial y}\right) - G_{13}\frac{\partial^2\phi_x^*}{\partial x^2} - G_{33}\left(\frac{\partial^2\phi_x^*}{\partial x\partial y} + \frac{\partial^2\phi_y^*}{\partial x^2}\right)\\
&+ I_{44}\left(\phi_y + \frac{\partial w_0}{\partial y}\right) + I_{45}\left(\phi_x + \frac{\partial w_0}{\partial x}\right) + 3K_{44}\phi_y^* + 3K_{45}\phi_x^* = I_1\ddot{v}_0 + I_2\ddot{\phi}_y + I_4\ddot{\phi}_y^*, \qquad (45e)\\
&- E_{11}\frac{\partial^2 u_0}{\partial x^2} - E_{12}\frac{\partial^2 v_0}{\partial x\partial y} - E_{13}\left(2\frac{\partial^2 u_0}{\partial x\partial y} + \frac{\partial^2 v_0}{\partial x^2}\right) - E_{23}\frac{\partial^2 v_0}{\partial y^2} - E_{33}\left(\frac{\partial^2 u_0}{\partial y^2} + \frac{\partial^2 v_0}{\partial x\partial y}\right)\\
&- G_{11}\frac{\partial^2\phi_x}{\partial x^2} - G_{12}\frac{\partial^2\phi_y}{\partial x\partial y} - G_{13}\left(2\frac{\partial^2\phi_x}{\partial x\partial y} + \frac{\partial^2\phi_y}{\partial x^2}\right) - G_{23}\frac{\partial^2\phi_y}{\partial y^2} - G_{33}\left(\frac{\partial^2\phi_x}{\partial y^2} + \frac{\partial^2\phi_y}{\partial x\partial y}\right)\\
&- H_{11}\frac{\partial^2\phi_x^*}{\partial x^2} - H_{12}\frac{\partial^2\phi_y^*}{\partial x\partial y} - H_{13}\left(2\frac{\partial^2\phi_x^*}{\partial x\partial y} + \frac{\partial^2\phi_y^*}{\partial x^2}\right) - H_{23}\frac{\partial^2\phi_y^*}{\partial y^2} - H_{33}\left(\frac{\partial^2\phi_x^*}{\partial y^2} + \frac{\partial^2\phi_y^*}{\partial x\partial y}\right)\\
&+ 3K_{45}\left(\phi_y + \frac{\partial w_0}{\partial y}\right) + 3K_{55}\left(\phi_x + \frac{\partial w_0}{\partial x}\right) + 9L_{45}\phi_y^* + 9L_{55}\phi_x^* = I_3\ddot{u}_0 + I_4\ddot{\phi}_x + I_6\ddot{\phi}_x^*, \qquad (45f)\\
&- E_{12}\frac{\partial^2 u_0}{\partial x\partial y} - E_{22}\frac{\partial^2 v_0}{\partial y^2} - E_{23}\left(\frac{\partial^2 u_0}{\partial y^2} + 2\frac{\partial^2 v_0}{\partial x\partial y}\right) - E_{13}\frac{\partial^2 u_0}{\partial x^2} - E_{33}\left(\frac{\partial^2 u_0}{\partial x\partial y} + \frac{\partial^2 v_0}{\partial x^2}\right)\\
&- G_{12}\frac{\partial^2\phi_x}{\partial x\partial y} - G_{22}\frac{\partial^2\phi_y}{\partial y^2} - G_{23}\left(\frac{\partial^2\phi_x}{\partial y^2} + 2\frac{\partial^2\phi_y}{\partial x\partial y}\right) - G_{13}\frac{\partial^2\phi_x}{\partial x^2} - G_{33}\left(\frac{\partial^2\phi_x}{\partial x\partial y} + \frac{\partial^2\phi_y}{\partial x^2}\right)\\
&- H_{12}\frac{\partial^2\phi_x^*}{\partial x\partial y} - H_{22}\frac{\partial^2\phi_y^*}{\partial y^2} - H_{23}\left(\frac{\partial^2\phi_x^*}{\partial y^2} + 2\frac{\partial^2\phi_y^*}{\partial x\partial y}\right) - H_{13}\frac{\partial^2\phi_x^*}{\partial x^2} - H_{33}\left(\frac{\partial^2\phi_x^*}{\partial x\partial y} + \frac{\partial^2\phi_y^*}{\partial x^2}\right)\\
&+ 3K_{44}\left(\phi_y + \frac{\partial w_0}{\partial y}\right) + 3K_{45}\left(\phi_x + \frac{\partial w_0}{\partial x}\right) + 9L_{44}\phi_y^* + 9L_{45}\phi_x^* = I_3\ddot{v}_0 + I_4\ddot{\phi}_y + I_6\ddot{\phi}_y^*. \qquad (45g)
\end{aligned}
$$

Appendix B

This appendix presents the equations of motion to be interpolated by radial basis functions.

$$
\begin{aligned}
&- A_{11}\frac{\partial^2 U}{\partial x^2} - A_{12}\frac{\partial^2 V}{\partial x\partial y} - A_{13}\left(2\frac{\partial^2 V}{\partial x\partial y} + \frac{\partial^2 V}{\partial x^2}\right) - A_{23}\frac{\partial^2 V}{\partial y^2} - A_{33}\left(\frac{\partial^2 U}{\partial y^2} + \frac{\partial^2 V}{\partial x\partial y}\right)\\
&- B_{11}\frac{\partial^2\Psi_x}{\partial x^2} - B_{12}\frac{\partial^2\Psi_y}{\partial x\partial y} - B_{13}\left(2\frac{\partial^2\Psi_x}{\partial x\partial y} + \frac{\partial^2\phi_y}{\partial x^2}\right) - B_{23}\frac{\partial^2\phi_y}{\partial y^2} - B_{33}\left(\frac{\partial^2\phi_x}{\partial y^2} + \frac{\partial^2\phi_y}{\partial x\partial y}\right)\\
&- E_{11}\frac{\partial^2\Psi_x^*}{\partial x^2} - E_{12}\frac{\partial^2\Psi_y^*}{\partial x\partial y} - E_{13}\left(2\frac{\partial^2\Psi_x^*}{\partial x\partial y} + \frac{\partial^2\Psi_y^*}{\partial x^2}\right) - E_{23}\frac{\partial^2\Psi_y^*}{\partial y^2} - E_{33}\left(\frac{\partial^2\Psi_x^*}{\partial y^2} + \frac{\partial^2\Psi_y^*}{\partial x\partial y}\right)\\
&= -(I_0\omega^2 U + I_1\omega^2\Psi_x + I_3\omega^2\Psi_x^*), \qquad (46a)\\
&- A_{12}\frac{\partial^2 U}{\partial x\partial y} - A_{22}\frac{\partial^2 V}{\partial y^2} - A_{23}\left(\frac{\partial^2 U}{\partial y^2} + 2\frac{\partial^2 V}{\partial x\partial y}\right) - A_{13}\frac{\partial^2 U}{\partial x^2} - A_{33}\left(\frac{\partial^2 U}{\partial x\partial y} + \frac{\partial^2 V}{\partial x^2}\right)\\
&- B_{12}\frac{\partial^2\Psi_x}{\partial x\partial y} - B_{22}\frac{\partial^2\Psi_y}{\partial y^2} - B_{23}\left(\frac{\partial^2\Psi_x}{\partial y^2} + 2\frac{\partial^2\Psi_y}{\partial x\partial y}\right) - B_{13}\frac{\partial^2\Psi_x}{\partial x^2} - B_{33}\left(\frac{\partial^2\Psi_x}{\partial x\partial y} + \frac{\partial^2\Psi_y}{\partial x^2}\right)\\
&- E_{12}\frac{\partial^2\Psi_x^*}{\partial x\partial y} - E_{22}\frac{\partial^2\Psi_y^*}{\partial y^2} - E_{23}\left(\frac{\partial^2\Psi_x^*}{\partial y^2} + 2\frac{\partial^2\Psi_y^*}{\partial x\partial y}\right) - E_{13}\frac{\partial^2\Psi_x^*}{\partial x^2} - E_{33}\left(\frac{\partial^2\Psi_x^*}{\partial x\partial y} + \frac{\partial^2\Psi_y^*}{\partial x^2}\right)\\
&= -(I_0\omega^2 V + I_1\omega^2\Psi_y + I_3\omega^2\Psi_y^*), \qquad (46b)
\end{aligned}
$$

$$- I_{44}\left(\frac{\partial \Psi_y}{\partial y}+\frac{\partial^2 W}{\partial y^2}\right) - I_{45}\left(\frac{\partial \Psi_x}{\partial y}+2\frac{\partial^2 W}{\partial x \partial y}+\frac{\partial \Psi_y}{\partial x}\right) - I_{55}\left(\frac{\partial \Psi_x}{\partial x}+\frac{\partial^2 W}{\partial x^2}\right) - 3K_{44}\frac{\partial \Psi_y^*}{\partial y} - 3K_{45}\left(\frac{\partial \Psi_x^*}{\partial y}+\frac{\partial \Psi_y^*}{\partial x}\right) - 3K_{55}\frac{\partial \Psi_x^*}{\partial x} = -I_0\omega^2 W, \tag{46c}$$

$$\begin{aligned} &- B_{11}\frac{\partial^2 U}{\partial x^2} - B_{12}\frac{\partial^2 V}{\partial x \partial y} - B_{13}\left(2\frac{\partial^2 U}{\partial x \partial y}+\frac{\partial^2 V}{\partial x^2}\right) - B_{23}\frac{\partial^2 V}{\partial y^2} - B_{33}\left(\frac{\partial^2 U}{\partial y^2}+\frac{\partial^2 V}{\partial x \partial y}\right) \\ &- F_{11}\frac{\partial^2 \Psi_x}{\partial x^2} - F_{12}\frac{\partial^2 \Psi_y}{\partial x \partial y} - F_{13}\left(2\frac{\partial^2 \Psi_x}{\partial x \partial y}+\frac{\partial^2 \Psi_y}{\partial x^2}\right) - F_{23}\frac{\partial^2 \Psi_y}{\partial y^2} - F_{33}\left(\frac{\partial^2 \Psi_x}{\partial y^2}+\frac{\partial^2 \Psi_y}{\partial x \partial y}\right) \\ &- G_{11}\frac{\partial^2 \Psi_x^*}{\partial x^2} - G_{12}\frac{\partial^2 \Psi_y^*}{\partial x \partial y} - G_{13}\left(2\frac{\partial^2 \Psi_x^*}{\partial x \partial y}+\frac{\partial^2 \Psi_y^*}{\partial x^2}\right) - G_{23}\frac{\partial^2 \Psi_y^*}{\partial y^2} - G_{33}\left(\frac{\partial^2 \Psi_x^*}{\partial y^2}+\frac{\partial^2 \Psi_y^*}{\partial x \partial y}\right) \\ &+ I_{45}\left(\Psi_y+\frac{\partial W}{\partial y}\right) + I_{55}\left(\Psi_x+\frac{\partial W}{\partial x}\right) + 3K_{45}\Psi_y^* + 3K_{55}\phi_x^* = -(I_1\omega^2 U + I_2\omega^2\Psi_x + I_4\omega^2\Psi_x^*), \end{aligned} \tag{46d}$$

$$\begin{aligned} &- B_{12}\frac{\partial^2 U}{\partial x \partial y} - B_{22}\frac{\partial^2 V}{\partial y^2} - B_{23}\left(\frac{\partial^2 U}{\partial y^2}+2\frac{\partial^2 V}{\partial x \partial y}\right) - B_{13}\frac{\partial^2 U}{\partial x^2} - B_{33}\left(\frac{\partial^2 U}{\partial x \partial y}+\frac{\partial^2 V}{\partial x^2}\right) \\ &- F_{12}\frac{\partial^2 \Psi_x}{\partial x \partial y} - F_{22}\frac{\partial^2 \Psi_y}{\partial y^2} - F_{23}\left(\frac{\partial^2 \Psi_x}{\partial y^2}+2\frac{\partial^2 \Psi_y}{\partial x \partial y}\right) - F_{13}\frac{\partial^2 \Psi_x}{\partial x^2} - F_{33}\left(\frac{\partial^2 \Psi_x}{\partial x \partial y}+\frac{\partial^2 \Psi_y}{\partial x^2}\right) \\ &- G_{12}\frac{\partial^2 \Psi_x^*}{\partial x \partial y} - G_{22}\frac{\partial^2 \Psi_y^*}{\partial y^2} - G_{23}\left(\frac{\partial^2 \Psi_x^*}{\partial y^2}+2\frac{\partial^2 \Psi_y^*}{\partial x \partial y}\right) - G_{13}\frac{\partial^2 \Psi_x^*}{\partial x^2} - G_{33}\left(\frac{\partial^2 \Psi_x^*}{\partial x \partial y}+\frac{\partial^2 \Psi_y^*}{\partial x^2}\right) \\ &+ I_{44}\left(\Psi_y+\frac{\partial W}{\partial y}\right) + I_{45}\left(\Psi_x+\frac{\partial W}{\partial x}\right) + 3K_{44}\Psi_y^* + 3K_{45}\Psi_x^* = -(I_1\omega^2 V + I_2\omega^2\Psi_y + I_4\omega^2\Psi_y^*), \end{aligned} \tag{46e}$$

$$\begin{aligned} &- E_{11}\frac{\partial^2 U}{\partial x^2} - E_{12}\frac{\partial^2 V}{\partial x \partial y} - E_{13}\left(2\frac{\partial^2 U}{\partial x \partial y}+\frac{\partial^2 V}{\partial x^2}\right) - E_{23}\frac{\partial^2 V}{\partial y^2} - E_{33}\left(\frac{\partial^2 U}{\partial y^2}+\frac{\partial^2 V}{\partial x \partial y}\right) \\ &- G_{11}\frac{\partial^2 \Psi_x}{\partial x^2} - G_{12}\frac{\partial^2 \Psi_y}{\partial x \partial y} - G_{13}\left(2\frac{\partial^2 \Psi_x}{\partial x \partial y}+\frac{\partial^2 \Psi_y}{\partial x^2}\right) - G_{23}\frac{\partial^2 \Psi_y}{\partial y^2} - G_{33}\left(\frac{\partial^2 \Psi_x}{\partial y^2}+\frac{\partial^2 \Psi_y}{\partial x \partial y}\right) \\ &- H_{11}\frac{\partial^2 \Psi_x^*}{\partial x^2} - H_{12}\frac{\partial^2 \Psi_y^*}{\partial x \partial y} - H_{13}\left(2\frac{\partial^2 \Psi_x^*}{\partial x \partial y}+\frac{\partial^2 \Psi_y^*}{\partial x^2}\right) - H_{23}\frac{\partial^2 \Psi_y^*}{\partial y^2} - H_{33}\left(\frac{\partial^2 \Psi_x^*}{\partial y^2}+\frac{\partial^2 \Psi_y^*}{\partial x \partial y}\right) \\ &+ 3K_{45}\left(\phi_y+\frac{\partial W}{\partial y}\right) + 3K_{55}\left(\Psi_x+\frac{\partial W}{\partial x}\right) + 9L_{45}\Psi_y^* + 9L_{55}\Psi_x^* = -(I_3\omega^2 U + I_4\omega^2\Psi_x + I_6\omega^2\Psi_x^*), \end{aligned} \tag{46f}$$

$$\begin{aligned} &- E_{12}\frac{\partial^2 U}{\partial x \partial y} - E_{22}\frac{\partial^2 V}{\partial y^2} - E_{23}\left(\frac{\partial^2 U}{\partial y^2}+2\frac{\partial^2 V}{\partial x \partial y}\right) - E_{13}\frac{\partial^2 U}{\partial x^2} - E_{33}\left(\frac{\partial^2 U}{\partial x \partial y}+\frac{\partial^2 V}{\partial x^2}\right) \\ &- G_{12}\frac{\partial^2 \Psi_x}{\partial x \partial y} - G_{22}\frac{\partial^2 \Psi_y}{\partial y^2} - G_{23}\left(\frac{\partial^2 \Psi_x}{\partial y^2}+2\frac{\partial^2 \Psi_y}{\partial x \partial y}\right) - G_{13}\frac{\partial^2 \Psi_x}{\partial x^2} - G_{33}\left(\frac{\partial^2 \Psi_x}{\partial x \partial y}+\frac{\partial^2 \Psi_y}{\partial x^2}\right) \\ &- H_{12}\frac{\partial^2 \Psi_x^*}{\partial x \partial y} - H_{22}\frac{\partial^2 \Psi_y^*}{\partial y^2} - H_{23}\left(\frac{\partial^2 \Psi_x^*}{\partial y^2}+2\frac{\partial^2 \Psi_y^*}{\partial x \partial y}\right) - H_{13}\frac{\partial^2 \Psi_x^*}{\partial x^2} - H_{33}\left(\frac{\partial^2 \Psi_x^*}{\partial x \partial y}+\frac{\partial^2 \Psi_y^*}{\partial x^2}\right) \\ &+ 3K_{44}\left(\Psi_y+\frac{\partial W}{\partial y}\right) + 3K_{45}\left(\Psi_x+\frac{\partial W}{\partial x}\right) + 9L_{44}\Psi_y^* + 9L_{45}\Psi_x^* = -(I_3\omega^2 V + I_4\omega^2\Psi_y + I_6\omega^2\Psi_y^*), \end{aligned} \tag{46g}$$

where stiffness components are given as

$$A_{ij}, B_{ij}, E_{ij}, F_{ij}, G_{ij}, H_{ij} = \overline{Q}_{ij} \int_{-h/2}^{h/2} (1, z, z^3, z^2, z^4, z^6)\, \mathrm{d}z \quad i,j = 1,2,3, \tag{47}$$

$$I_{ij}, K_{ij}, L_{ij} = \overline{Q}_{ij} \int_{-h/2}^{h/2} (1, z^2, z^4)\, \mathrm{d}z \quad i,j = 4,5. \tag{48}$$

References

[1] R.L. Hardy, Multiquadric equations of topography and other irregular surfaces, *Geophysical Research* 176 (1971) 1905–1915.
[2] R.L. Hardy, Theory and applications of the multiquadric-biharmonic method: 20 years of discovery, *Computers and Mathematics with Applications* 19 (8/9) (1990) 163–208.
[3] E.J. Kansa, Multiquadrics—a scattered data approximation scheme with applications to computational fluid dynamics, I: surface approximations and partial derivative estimates, *Computers and Mathematics with Applications* 19 (8/9) (1990) 127–145.
[4] E.J. Kansa, Multiquadrics—a scattered data approximation scheme with applications to computational fluid dynamics, II: solutions to parabolic, hyperbolic and elliptic partial differential equations, *Computers and Mathematics with Applications* 19 (8/9) (1990) 147–161.
[5] G.R. Liu, *Mesh Free Methods*, CRC Press, Boca Raton, USA, 2003.
[6] M.J.D. Powell, The theory of radial basis function approximation in 1990, in: F.W. Light (Ed.), *Advances in Numerical Analysis*, Oxford University Press, Oxford, 1992, pp. 203–240.
[7] C.J. Coleman, On the use of radial basis functions in the solution of elliptic boundary value problems, *Computational Mechanics* 17 (1996) 418–422.
[8] M. Sharan, E.J. Kansa, S. Gupta, Application of the multiquadric method for numerical solution of elliptic partial differential equations, *Applied Mathematics and Computations* 84 (1997) 275–302.
[9] H. Wendland, Error estimates for interpolation by compactly supported radial basis functions of minimal degree, *Journal of Approximation Theory* 93 (1998) 258–296.
[10] Y.C. Hon, M.W. Lu, W.M. Xue, Y.M. Zhu, Multiquadric method for the numerical solution of byphasic mixture model, *Applied Mathematics and Computations* 88 (1997) 153–175.
[11] Y.C. Hon, K.F. Cheung, X.Z. Mao, E.J. Kansa, A multiquadric solution for the shallow water equation, *ASCE Journal of Hydraulic Engineering* 125 (5) (1999) 524–533.
[12] J.G. Wang, G.R. Liu, P. Lin, Numerical analysis of biot's consolidation process by radial point interpolation method, *International Journal of Solids and Structures* 39 (6) (2002) 1557–1573.
[13] A.J.M. Ferreira, A formulation of the multiquadric radial basis function method for the analysis of laminated composite plates, *Composite Structures* 59 (2003) 385–392.
[14] A.J.M. Ferreira, C.M.C. Roque, P.A.L.S. Martins, Analysis of composite plates using higher-order shear deformation theory and a finite point formulation based on the multiquadric radial basis function method, *Composites: Part B* 34 (2003) 627–636.
[15] A.J.M. Ferreira, R.C. Batra, C.M.C. Roque, L.F. Qian, P.A.L.S. Martins, Static analysis of functionally graded plates using third-order shear deformation theory and a meshless method, *Composite Structures* 69 (2005) 449–457.
[16] M.B. Bever, P.E. Duwez, Gradients in composite materials, *Materials Science and Engineering* 10 (1972) 1–8.
[17] F.J. Ferrante, L.L. Graham-Brady, Stochastic simulation of non-Gaussian/non-stationary properties in a functionally graded plate, *Computer Methods in Applied Mechanics and Engineering* 194 (12–16) (2005) 1675–1692.
[18] H.M. Yin, L.Z. Sun, G.H. Paulino, Micromechanics-based elastic model for functionally graded materials with particle interactions, *Acta Materialia* 52 (12) (2004) 3535–3543.
[19] J.N. Reddy, *Mechanics of Laminated Composite Plates: Theory and Analysis*, CRC Press, Boca Raton, FL, 2003.
[20] B.N. Pandya, T. Kant, Higher-order shear deformable theories for flexure of sandwich plates-finite element evaluations, *International Journal of Solids and Structures* 24 (1988) 419–451.
[21] H. Arya, R.P. Shimpi, N.K. Naik, A zigzag model for laminated composite beams, *Composite structures* 56 (2002) 21–24.
[22] E.J. Kansa, Y.C. Hon, Circumvecting the ill-conditioning problem with multiquadric radial basis functions, *Computers and Mathematics with Applications* 39 (7–8) (2000) 123–137.
[23] G.E. Fasshauer, Solving partial differential equations by collocation with radial basis functions, in: *Surface Fitting and Multiresolution Methods, Vol. 2: Proceedings of the Third International Conference on Curves and Surfaces*, vol. 2, 1997, pp. 131–138.
[24] Y.C. Hon, X.Z. Mao, On unsymmetric collocation by radial basis functions, *Applied Mathematics and Computations* 119 (2–3) (2001) 177–186.
[25] R.K. Beatson, Fast fitting of radial basis functions: methods based on preconditioned gmres iteration, *Advances in Computational Mathematics* 11 (1999) 253–270.
[26] Y.C. Hon, L. Ling, K.M. Liew, Numerical analysis of parameters in a laminated beam model by radial basis functions, *Computers Materials and Continua* 2 (1) (2005) 39–49.

[27] Y. Liu, K.M. Liew, Y.C. Hon, X. Zhang, Numerical simulation of an electroactuated beam using a radial basis function, *Smart Materials and Structures* 14 (2005) 1163–1171.
[28] S. Rippa, An algorithm for selecting a good value for the parameter c in radial basis function interpolation, *Advances in Computational Mathematics* 11 (1999) 193–210.
[29] T. Mori, K. Tanaka, Average stress in matrix and average elastic energy of materials with misfitting inclusions, *Acta Metallurgica* 21 (1973) 571–574.
[30] A.J.M. Ferreira, R.C. Batra, C.M.C. Roque, L.F. Qian, R.M.N. Jorge, Natural frequencies of functionally graded plates by a meshless method, *Composite Structures* 75 (2006) 593–600.
[31] S.S. Vel, R.C. Batra, Three-dimensional exact solution for the vibration of functionally graded rectangular plates, *Journal of Sound and Vibration* (272) (2004) 703–730.
[32] J.N. Reddy, A simple higher-order theory for laminated composite plates, *Journal of Applied Mechanics* 51 (1984) 745–775.